Science des Procédés Céramiques et de Traitements de Surface
UMR CNRS 7315

3rd Iranian Refractory Symposium
special focus on
Challenges Against Contribution to Overseas Market
Organizer
Iran Refractory Society
In collaboration with
Iran Mine House & Iran Ceramic Society

Axe 4 - Ceramics under environmental stresses

Relationship between microstructure and thermomechanical behaviour. Measurement of these properties and interpretation with the help of model materials

Prof. Marc HUGER
University of Limoges, France
Leader of TMC research group at SPCTS
(Thermo-Mechanics on Ceramics)

Université de Limoges

cnrs

Outlines

➔ Analytical methods for continuum micromechanics

➔ Useful analytical bounds for prediction of effective properties of random media

➔ Numerical approaches for continuum micromechanics (homogenization techniques)

➔ Concepts will be applied both on model refractory materials and industrial ones

➔ A focus on the influence of CTE mismatch between constituents

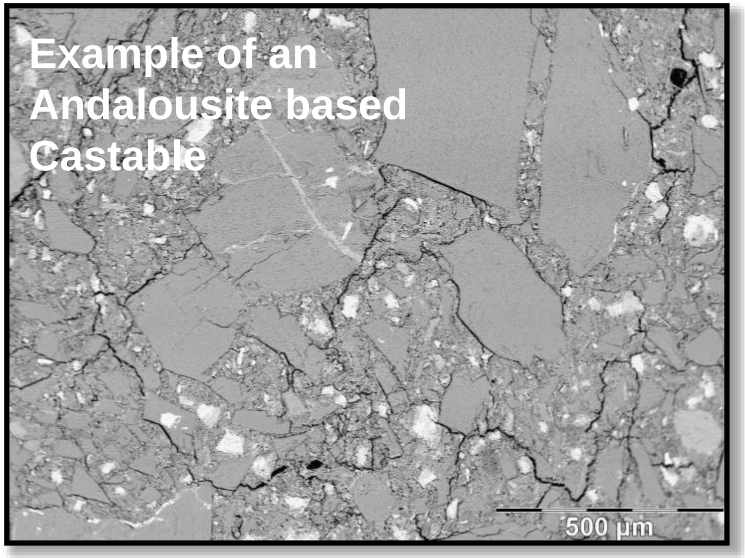

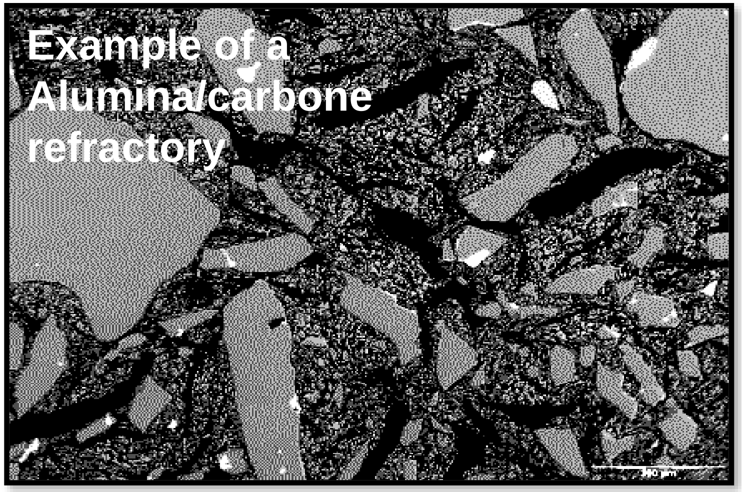

Université de Limoges
cnrs
SPC/TS Science des Procédés Céramiques et de Traitements de Surface
UMR CNRS 7315

Context of this lecture

Fracture Mechanics

LEFM …

$$K_{IC} = \sigma_r . \sqrt{\pi . a} = \sqrt{E . G_c} = \sqrt{E . (2 . \gamma_s)}$$

Flat R-Curve

… and deviations from it

$$G_f = 2 . \gamma_{wof} >> 2 . \gamma_s$$

Rising R-Curve, Low Brittleness

Thermal Shock Resistance

TSR : Stress criteria to crack initiation

$$R = \Delta T_c = \frac{\sigma_r . (1 - \nu)}{E . \alpha}$$

… for mild heat transfer conditions

$$R' = \lambda . R$$

TSR : Energy criteria to crack initiation

$$R'''' = \frac{\gamma_{wof}}{1/2 . (\sigma_r^2 / E)}$$

$$R_{st} = \sqrt{\frac{\gamma_{wof}}{\alpha^2 . E}}$$

… for mild heat transfer conditions

$$R_{st}^{'} = \lambda . R_{st}$$

➔ How to address effective properties ?

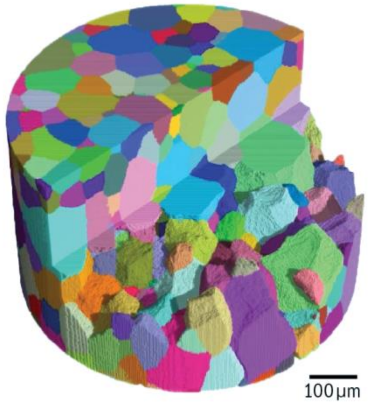

- **Thermal ones : α, λ**
- **Mechanical ones : E, σ= f(ε), σ_r, ε_r**

… from local scale **… to macro scale**

Different scales of interest

A dream of R&D Engineers: from raw materials to industrial device scale

- ➔ Individual local physic mechanisms quite easy to understand and then model
- ➔ Very heterogeneous systems in case of refractories
- ➔ Microstructure is subject to large evolutions during process and during use
- ➔ History of material should be taken into account

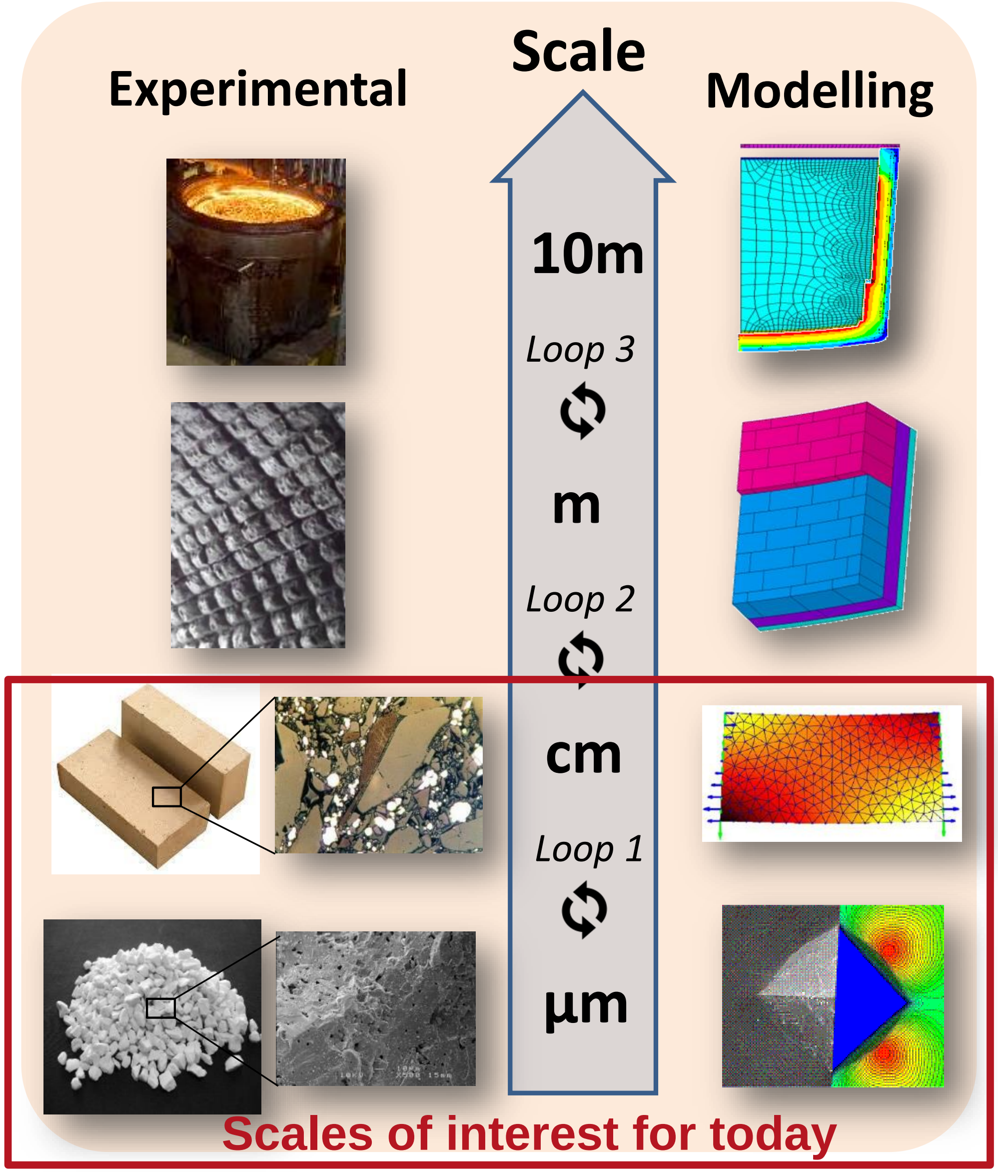

Reminder about simplifying the tensor notation

Hooke's law

$$\overline{\sigma}_{ij} = \overline{\overline{C}}_{ijkl} . \overline{\varepsilon}_{kl}$$

Indices can be replace as follows

$$\begin{bmatrix} 11 & 12 & 13 \\ 12 & 22 & 23 \\ 13 & 23 & 33 \end{bmatrix} \Rightarrow \begin{bmatrix} 1 & 6 & 5 \\ 6 & 2 & 4 \\ 5 & 4 & 3 \end{bmatrix}$$

… which allows to rewrite Hooke's law in a matrix format:

$$\overline{\sigma}_{I} = \overline{\overline{C}}_{IJ} . \overline{\varepsilon}_{J}$$

Tension-Compression Coupling

Tension-Compression

Shear

$$\begin{pmatrix} \sigma_1 \\ \sigma_2 \\ \sigma_3 \\ \sigma_4 \\ \sigma_5 \\ \sigma_6 \end{pmatrix} = \begin{pmatrix} C_{11} & C_{12} & C_{13} & C_{14} & C_{15} & C_{16} \\ C_{12} & C_{22} & C_{23} & C_{24} & C_{25} & C_{26} \\ C_{13} & C_{23} & C_{33} & C_{34} & C_{35} & C_{36} \\ C_{14} & C_{24} & C_{34} & C_{44} & C_{45} & C_{46} \\ C_{15} & C_{25} & C_{35} & C_{45} & C_{55} & C_{56} \\ C_{16} & C_{26} & C_{36} & C_{46} & C_{56} & C_{66} \end{pmatrix} \begin{pmatrix} \varepsilon_1 \\ \varepsilon_2 \\ \varepsilon_3 \\ \varepsilon_4 \\ \varepsilon_5 \\ \varepsilon_6 \end{pmatrix}$$

Tension-Compression

Shear

Often equals to zero

Note that…

$$\begin{bmatrix} \sigma_1 & \sigma_6 & \sigma_5 \\ \sigma_6 & \sigma_2 & \sigma_4 \\ \sigma_5 & \sigma_4 & \sigma_3 \end{bmatrix} = \begin{bmatrix} \sigma_{11} & \sigma_{12} & \sigma_{13} \\ \sigma_{12} & \sigma_{22} & \sigma_{23} \\ \sigma_{13} & \sigma_{23} & \sigma_{33} \end{bmatrix}$$

General case :

21 independents C_{IJ}

But…

$$\begin{bmatrix} \varepsilon_1 & \varepsilon_6 & \varepsilon_5 \\ \varepsilon_6 & \varepsilon_2 & \varepsilon_4 \\ \varepsilon_5 & \varepsilon_4 & \varepsilon_3 \end{bmatrix} = \begin{bmatrix} \varepsilon_{11} & 2.\varepsilon_{12} & 2.\varepsilon_{13} \\ 2.\varepsilon_{12} & \varepsilon_{22} & 2.\varepsilon_{23} \\ 2.\varepsilon_{13} & 2.\varepsilon_{23} & \varepsilon_{33} \end{bmatrix}$$

Elastic tensor from crystal symmetry (values in GPa)

Alumina (Al_2O_3)

Trigonal

➔ *6 independent C_{IJ}*

$$\begin{pmatrix} C_{11} & C_{12} & C_{13} & C_{14} & 0 & 0 \\ C_{12} & C_{11} & C_{13} & -C_{14} & 0 & 0 \\ C_{13} & C_{13} & C_{33} & 0 & 0 & 0 \\ C_{14} & -C_{14} & 0 & C_{44} & 0 & 0 \\ 0 & 0 & 0 & 0 & C_{44} & C_{14} \\ 0 & 0 & 0 & 0 & C_{14} & \frac{1}{2}(C_{11}-C_{12}) \end{pmatrix} = \begin{pmatrix} 497.2 & 162.8 & 116 & -21.9 & 0 & 0 \\ 162.8 & 497.2 & 116 & 21.9 & 0 & 0 \\ 116 & 116 & 500.8 & 0 & 0 & 0 \\ -21.9 & 21.9 & 0 & 146.7 & 0 & 0 \\ 0 & 0 & 0 & 0 & 146.7 & -21.9 \\ 0 & 0 & 0 & 0 & -21.9 & 167.2 \end{pmatrix}$$

From O.L.Anderson et al., Elastic constants of mantle minerals at high temperature. Handbook of Physical Constants (1995)

Silica (SiO_2)

Vitreous (isotropic)

➔ *2 independent C_{IJ}*

$$\begin{pmatrix} C_{11} & C_{11}-2.C_{44} & C_{11}-2.C_{44} & 0 & 0 & 0 \\ C_{11}-2.C_{44} & C_{11} & C_{11}-2.C_{44} & 0 & 0 & 0 \\ C_{11}-2.C_{44} & C_{11}-2.C_{44} & C_{11} & 0 & 0 & 0 \\ 0 & 0 & 0 & C_{44} & 0 & 0 \\ 0 & 0 & 0 & 0 & C_{44} & 0 \\ 0 & 0 & 0 & 0 & 0 & C_{44} \end{pmatrix} = \begin{pmatrix} 78.5 & 16.1 & 16.1 & 0 & 0 & 0 \\ 16.1 & 78.5 & 16.1 & 0 & 0 & 0 \\ 16.1 & 16.1 & 78.5 & 0 & 0 & 0 \\ 0 & 0 & 0 & 31.2 & 0 & 0 \\ 0 & 0 & 0 & 0 & 31.2 & 0 \\ 0 & 0 & 0 & 0 & 0 & 31.2 \end{pmatrix}$$

From B.A.Auld, Acoustic fields and waves in solids, vol.1, Wiley, New York, (1973)

Mullite ($3Al_2O_3.2SiO_2$)

Orthorhombic

➔ *9 independent C_{IJ}*

$$\begin{pmatrix} C_{11} & C_{12} & C_{13} & 0 & 0 & 0 \\ C_{12} & C_{22} & C_{23} & 0 & 0 & 0 \\ C_{13} & C_{23} & C_{33} & 0 & 0 & 0 \\ 0 & 0 & 0 & C_{44} & 0 & 0 \\ 0 & 0 & 0 & 0 & C_{55} & 0 \\ 0 & 0 & 0 & 0 & 0 & C_{66} \end{pmatrix} = \begin{pmatrix} 291.3 & 112.9 & 96.2 & 0 & 0 & 0 \\ 112.9 & 232.9 & 121.9 & 0 & 0 & 0 \\ 96.2 & 121.9 & 352.1 & 0 & 0 & 0 \\ 0 & 0 & 0 & 110.3 & 0 & 0 \\ 0 & 0 & 0 & 0 & 77.4 & 0 \\ 0 & 0 & 0 & 0 & 0 & 79.9 \end{pmatrix}$$

From B. Hildmann, H. Ledbetter, S. Kim, H. Schneider, J. Am. Ceram. Soc., 84 [10] 2409–14 (2001)

Elastic tensor from crystal symmetry (values in GPa)

Magnesia (MgO)

Cubic

➔ *3 independent C_{IJ}*

$$\begin{pmatrix} C_{11} & C_{12} & C_{12} & 0 & 0 & 0 \\ C_{12} & C_{11} & C_{12} & 0 & 0 & 0 \\ C_{12} & C_{12} & C_{11} & 0 & 0 & 0 \\ 0 & 0 & 0 & C_{44} & 0 & 0 \\ 0 & 0 & 0 & 0 & C_{44} & 0 \\ 0 & 0 & 0 & 0 & 0 & C_{44} \end{pmatrix} = \begin{pmatrix} 299 & 96.4 & 96.4 & 0 & 0 & 0 \\ 96.4 & 299 & 96.4 & 0 & 0 & 0 \\ 96.4 & 116 & 299 & 0 & 0 & 0 \\ 0 & 0 & 0 & 157.1 & 0 & 0 \\ 0 & 0 & 0 & 0 & 157.1 & 0 \\ 0 & 0 & 0 & 0 & 0 & 157.1 \end{pmatrix}$$

From O.L.Anderson et al., Elastic constants of mantle minerals at high temperature. Handbook of Physical Constants (1995)

Spinel ($MgAl_2O_4$)

Cubic

➔ *3 independent C_{IJ}*

$$\begin{pmatrix} C_{11} & C_{12} & C_{12} & 0 & 0 & 0 \\ C_{12} & C_{11} & C_{12} & 0 & 0 & 0 \\ C_{12} & C_{12} & C_{11} & 0 & 0 & 0 \\ 0 & 0 & 0 & C_{44} & 0 & 0 \\ 0 & 0 & 0 & 0 & C_{44} & 0 \\ 0 & 0 & 0 & 0 & 0 & C_{44} \end{pmatrix} = \begin{pmatrix} 292.2 & 168.7 & 168.7 & 0 & 0 & 0 \\ 168.7 & 292.2 & 168.7 & 0 & 0 & 0 \\ 168.7 & 168.7 & 292.2 & 0 & 0 & 0 \\ 0 & 0 & 0 & 156.5 & 0 & 0 \\ 0 & 0 & 0 & 0 & 156.5 & 0 \\ 0 & 0 & 0 & 0 & 0 & 156.5 \end{pmatrix}$$

From O.L.Anderson et al., Elastic constants of mantle minerals at high temperature. Handbook of Physical Constants (1995)

Andalusite ($Al_2O_3.SiO_2$)

Orthorhombic

➔ *9 independent C_{IJ}*

$$\begin{pmatrix} C_{11} & C_{12} & C_{13} & 0 & 0 & 0 \\ C_{12} & C_{22} & C_{23} & 0 & 0 & 0 \\ C_{13} & C_{23} & C_{33} & 0 & 0 & 0 \\ 0 & 0 & 0 & C_{44} & 0 & 0 \\ 0 & 0 & 0 & 0 & C_{55} & 0 \\ 0 & 0 & 0 & 0 & 0 & C_{66} \end{pmatrix} = \begin{pmatrix} 233.4 & 97.7 & 116.2 & 0 & 0 & 0 \\ 97.7 & 289 & 81.4 & 0 & 0 & 0 \\ 116.2 & 81.4 & 380.1 & 0 & 0 & 0 \\ 0 & 0 & 0 & 99.5 & 0 & 0 \\ 0 & 0 & 0 & 0 & 87.8 & 0 \\ 0 & 0 & 0 & 0 & 0 & 112.3 \end{pmatrix}$$

From R.L. Ralph et al., “Compressibility and Crystal Structure of Andalusite at High Pressures, Am. Mineral. (1984)

Stiffness of polycrystals estimated from single crystal

up-to 21 C_{IJ} | **For each grain** | **also 21 S_{IJ}**

$$\begin{pmatrix} C_{11} & C_{12} & C_{13} & C_{14} & C_{15} & C_{16} \\ C_{12} & C_{22} & C_{23} & C_{24} & C_{25} & C_{26} \\ C_{13} & C_{23} & C_{33} & C_{34} & C_{35} & C_{36} \\ C_{14} & C_{24} & C_{34} & C_{44} & C_{45} & C_{46} \\ C_{15} & C_{25} & C_{35} & C_{45} & C_{55} & C_{56} \\ C_{16} & C_{26} & C_{36} & C_{46} & C_{56} & C_{66} \end{pmatrix}$$

Stiffness

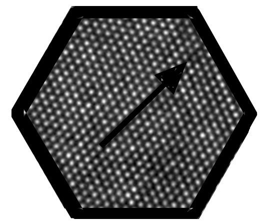

Compliance

$$\begin{pmatrix} S_{11} & S_{12} & S_{13} & S_{14} & S_{15} & S_{16} \\ S_{12} & S_{22} & S_{23} & S_{24} & S_{25} & S_{26} \\ S_{13} & S_{23} & S_{33} & S_{34} & S_{35} & S_{36} \\ S_{14} & S_{24} & S_{34} & S_{44} & S_{45} & S_{46} \\ S_{15} & S_{25} & S_{35} & S_{45} & S_{55} & S_{56} \\ S_{16} & S_{26} & S_{36} & S_{46} & S_{56} & S_{66} \end{pmatrix} = [C_{IJ}]^{-1}$$

For polycrystals ➔ AVERAGE

Voigt Average
(all grains undergo same strain)

$$E_V = \frac{(A - B + 3C).(A + 2B)}{2A + 3B + C}$$

$$G_V = \frac{(A - B + 3C)}{5}$$

with

$$A = \frac{C_{11} + C_{22} + C_{33}}{3}$$

$$B = \frac{C_{23} + C_{13} + C_{12}}{3}$$

$$C = \frac{C_{44} + C_{55} + C_{66}}{3}$$

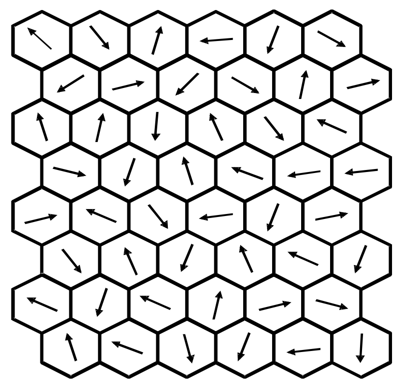

Reuss Average
(all grains undergo same stress)

$$E_R = \frac{5}{3A' + 2B' + C'}$$

$$G_R = \frac{5}{4A' - 4B' + 3C'}$$

with

$$A' = \frac{S_{11} + S_{22} + S_{33}}{3}$$

$$B' = \frac{S_{23} + S_{13} + S_{12}}{3}$$

$$C' = \frac{S_{44} + S_{55} + S_{66}}{3}$$

VRH : Hill Average
(between the two)

$$E_{VRH} = \frac{E_V + E_R}{2}$$

$$G_{VRH} = \frac{G_V + G_R}{2}$$

From R. Hill, The Elastic Behavior of a Crystalline Aggregate, Proc. Phys. Soc. Lond., (1952)

Stiffness of polycrystals estimated from single crystals

Note : Estimated without any porosity and without any defects

Material	E_V	E_R	E_{VRH}	G_V	G_R	G_{VRH}	ν_V	ν_R	ν_{VRH}
Alumina (Al_2O_3)	407.8	397.9	402.9	165.5	160.7	163.1	0.232	0.238	0.235
Silica (SiO_2)	73.0	73.0	73.0	31.2	31.2	31.2	0.170	0.170	0.170
Mullite ($3Al_2O_3.2SiO_2$)	229.4	220.0	224.7	89.9	85.9	87.9	0.276	0.281	0.279
Magnesia (MgO)	317.4	306.1	311.7	134.8	128.7	131.8	0.177	0.189	0.183
Spinel ($MgAl_2O_4$)	299.4	252.1	275.8	118.6	97.0	107.8	0.262	0.300	0.279
Andalusite ($Al_2O_3.SiO_2$)	250.6	241.0	245.8	100.4	96.4	98.4	0.248	0.250	0.249

Reminder:

$$\nu = \frac{E}{2.G} - 1$$ **is Poisson ratio**

$$K = \frac{E}{3.(1-2.\nu)}$$ **is Bulk modulus** **(not calculated here)**

Université de Limoges
cnrs
SPC/TS Science des Procédés Céramiques et de Traitements de Surface
UMR CNRS 7315

Effective elastic properties for "composite" materials with 2 constituents : VR approach (Voigt and Reuss)

In idealized case of a sandwich architecture (with perfect bonding):

- material 1 (isotropic): E_1, G_1, volume fraction v_1
- material 2 (isotropic): E_2, G_2, volume fraction v_2=1-v_1

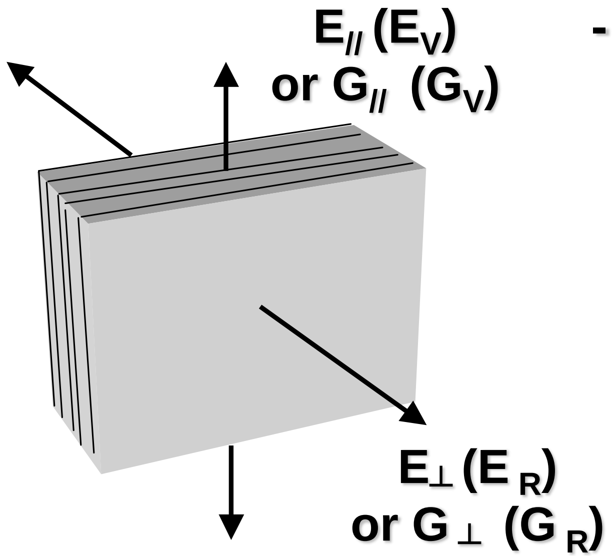

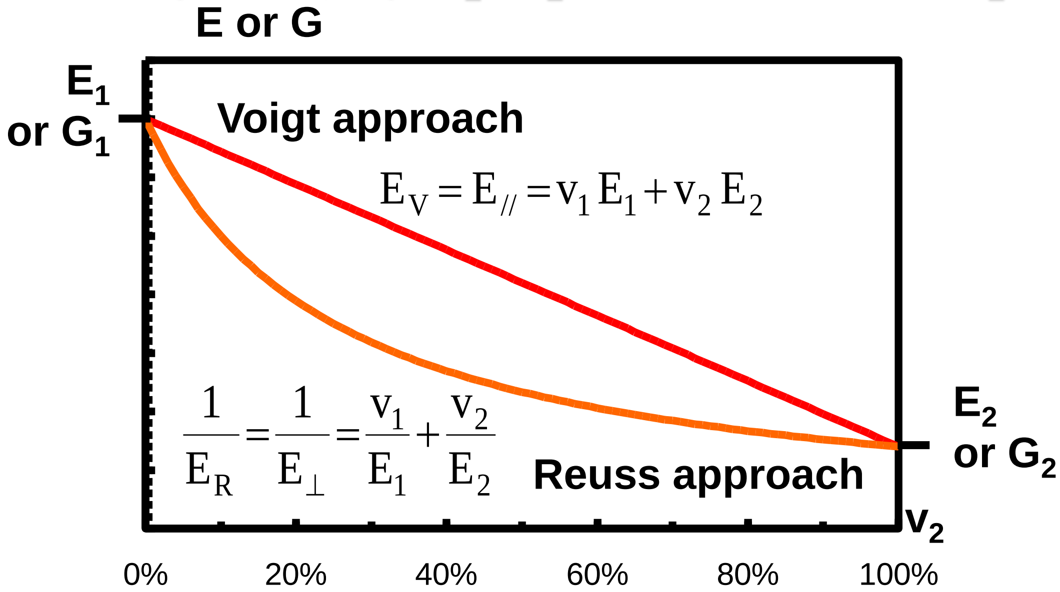

Note 1: Applicable for both G an E when materials exhibit quite similar ν values.

Note 2: Very easy to calculate and accurate in case of sandwich architecture. Result extremely dependent to the considered direction.

Note 3: Very extreme values between which every composite materials should be.

Note 4: Gap between the two can be rather large.

Effective elastic properties for "composite" materials with 2 constituents : HS approach (Hashin and Shtrikman)

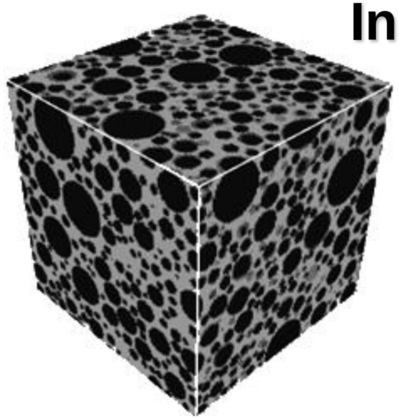

In case of a particulates composites (with perfect bonding):

- Matrix (isotropic): K_m, G_m, volume fraction v_m
- Particles (isotropic): K_p, G_p, volume fraction v_p=1-v_m

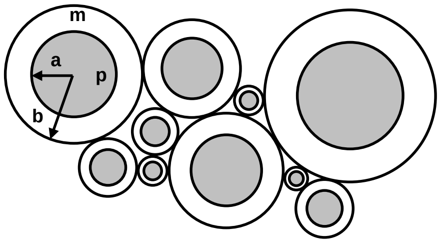

v_p adjusted by a/b ratio

➢ **Upper bound (HS+)**

$$K^{+} = K_p + \frac{v_m}{\dfrac{1}{K_m - K_p} + \dfrac{3v_p}{3K_p + 4G_p}}$$

$$G^{+} = G_p + \frac{v_m}{\dfrac{1}{G_m - G_p} + \dfrac{6(K_p + 2G_p) \cdot v_p}{5G_p(3K_p + 4G_p)}}$$

➔ $$E_{HS}^{+} = \frac{9K^{+} \cdot G^{+}}{3K^{+} + G^{+}}$$

➢ **Lower bound (HS-)**

$$K^{-} = K_m + \frac{v_p}{\dfrac{1}{K_p - K_m} + \dfrac{3v_m}{3K_m + 4G_m}}$$

$$G^{-} = G_m + \frac{v_p}{\dfrac{1}{G_p - G_m} + \dfrac{6(K_m + 2G_m) \cdot v_m}{5G_m(3K_m + 4G_m)}}$$

➔ $$E_{HS}^{-} = \frac{9K^{-} \cdot G^{-}}{3K^{-} + G^{-}}$$

Note 1: Lower bound (HS-) in case of hard particles in a soft matrix.

Note 2: Less easy to calculate, but very pertinent in most cases.

From Z. Hashin, Analysis of Composite Materials-A Survey, J. Appl. Mech., (1983)

Effective elastic properties for "composite" materials with 2 constituents : HS approach (Hashin and Shtrikman)

Example of alumina beads in a glass matrix (with perfect bonding):

- Matrix (Glass): E_m= 78GPa, ν_m=0,2 ➔ K_m, G_m
- Particles (Porous Alumina): E_p= 340GPa, ν_p=0,24 ➔ K_p, G_p

Cohesive interfaces

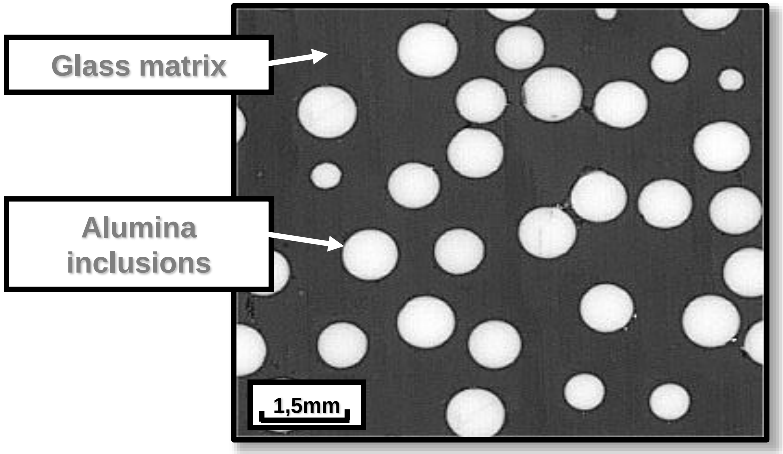

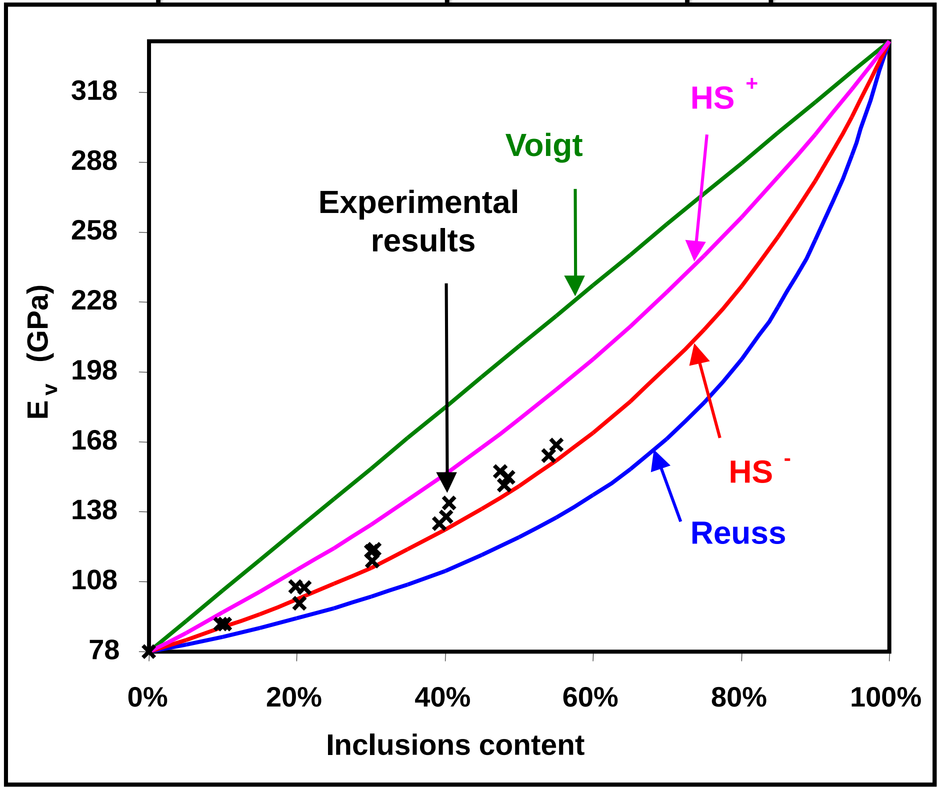

➔ **Hashin and Shtrikman's analytical model (HS-) is the most suitable one to estimate Young's modulus (with perfect bonding)**

From N. Tessier-Doyen, PhD, Limoges, (2003)

Effective elastic properties for “composite” materials with 2 constituents : FEM approach

Periodic homogenisation method ➔ **Faster convergence to the homogenised properties**

Periodic conditions:

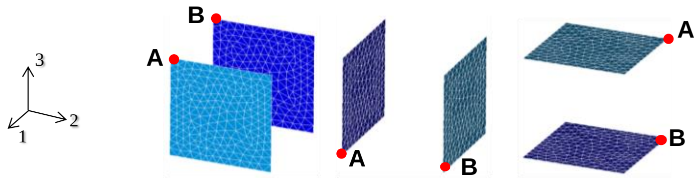

$$u_i(B) - u_i(A) = \bar{\varepsilon}_{ij} \cdot \left(x_j^B - x_j^A\right)$$

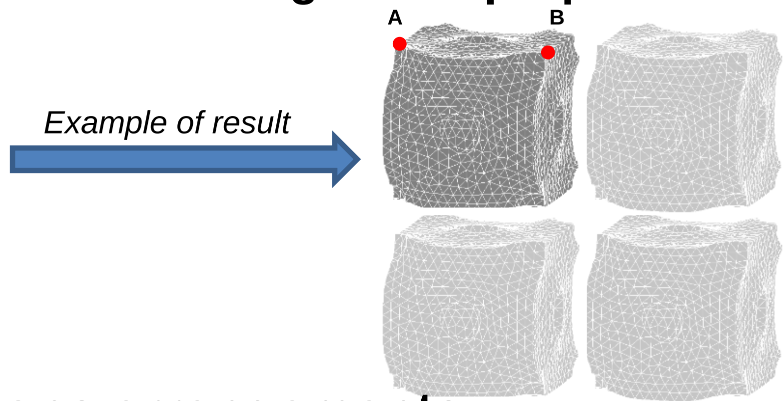

Quasi-isotropic periodic inclusions arrangements:

Find simple R.V.E. but as less anisotropic as possible

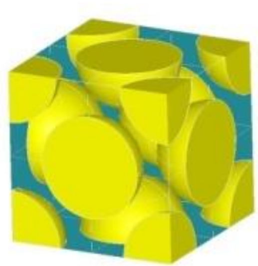

Face centred cubic arrangement

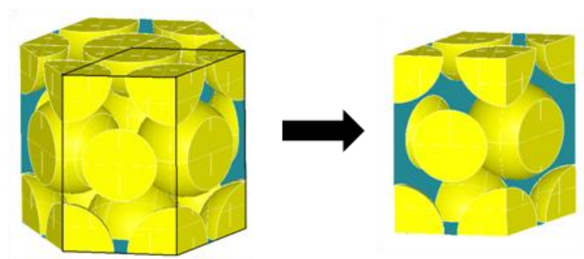

Hexagonal close packed arrangement

➔ Validation of these two periodic arrangements on Magnesia-Spinel materials

➔ **12 equivalent directions**

➔ **$\%_{inclusion} \leq 74\%$**

From R. Grasset-Bourdel, PhD, Leoben-Limoges, (2011)

Effective elastic properties for "composite" materials with 2 constituents : FEM approach

Example of alumina beads in a glass matrix (with perfect bonding):

- Matrix (Glass): E_m= 78GPa, ν_m=0,2 ➔K_m, G_m
- Particles (Porous Alumina): E_m= 340GPa, ν_m=0,24➔ K_p, G_p

Cohesive interfaces

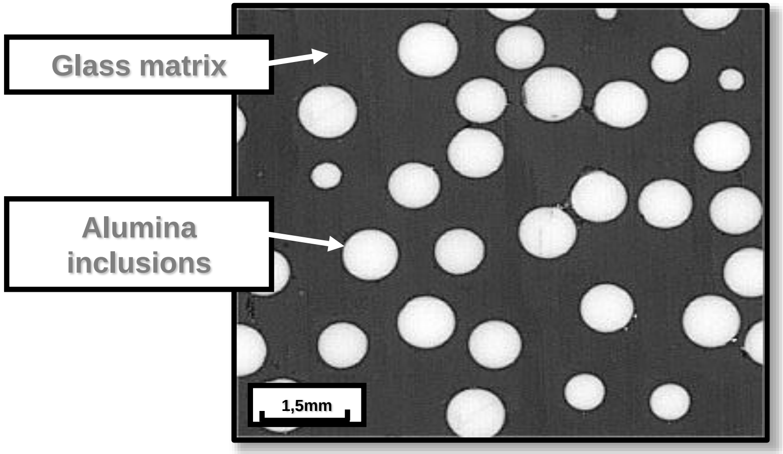

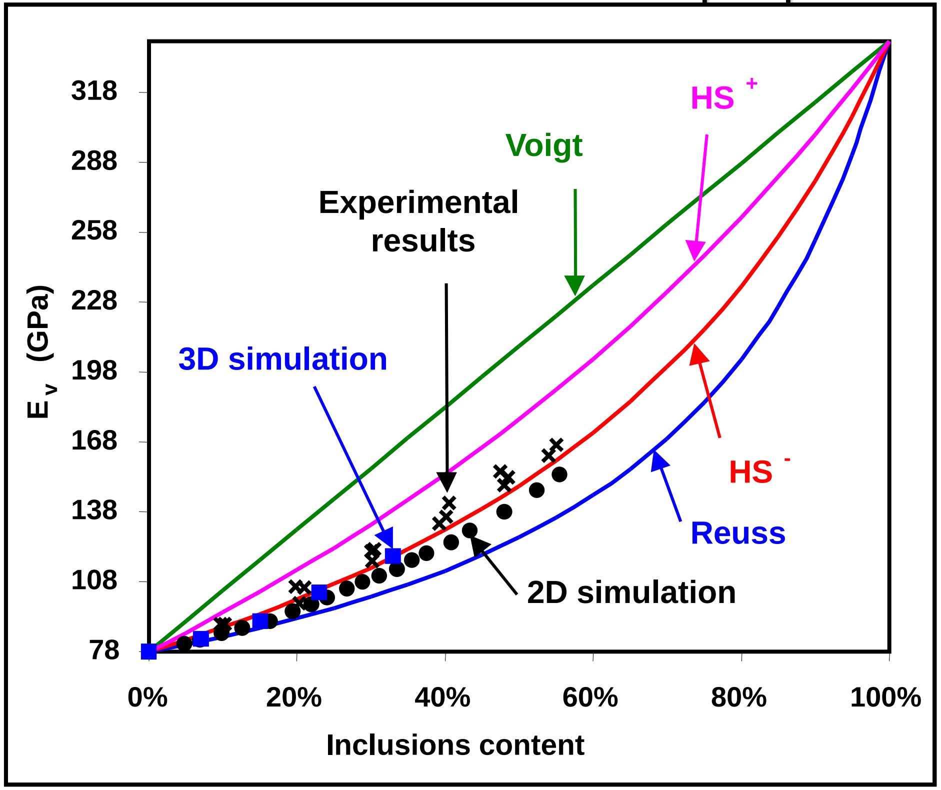

➔ **3D simulation using periodic homogenisation method is superimposed with Hashin and Shtrikman's analytical model (HS-)**

From N. Tessier-Doyen, PhD, Limoges, (2003)

Effective elastic properties for porous materials by analytical approaches

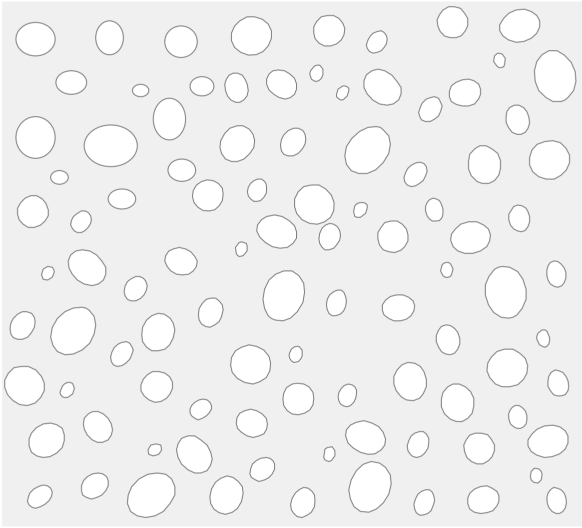

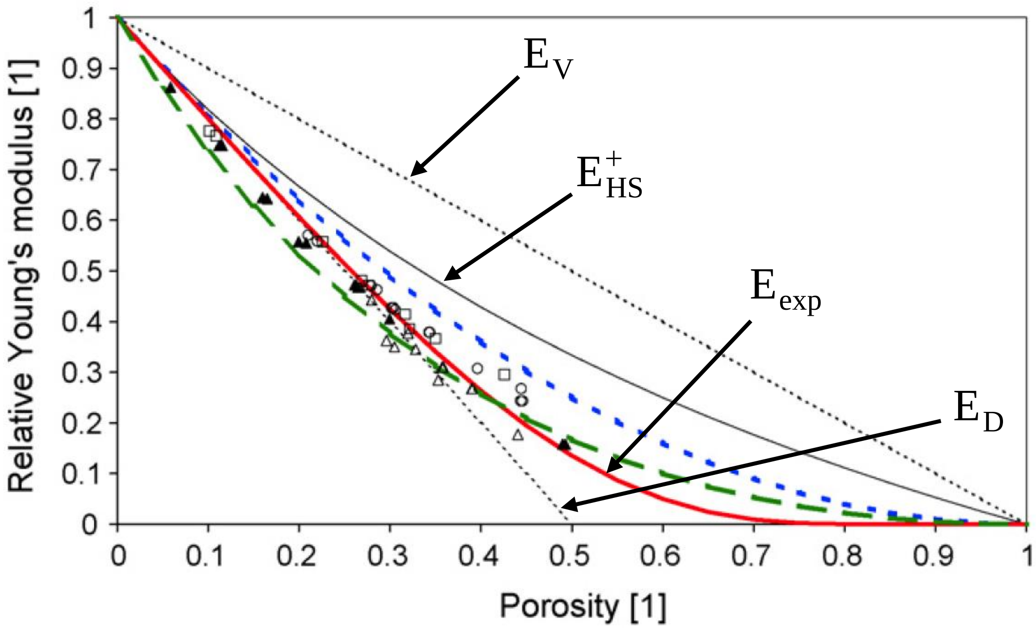

- **Voigt bound (V):** $E_V = E_o.(1 - v_p)$

- **Hashin and Shtrikman's bound (HS+):**

$$E^+_{HS} = E_o.\left(\frac{1 - v_p}{1 + v_p}\right)$$

- **Exponential relation (exp):**

$$E_{exp} = E_o.\exp\left(\frac{-2.v_p}{1 - v_p}\right)$$

- **Dilute limit approximation (D):** $E_D = E_o.(1 - 2.v_p)$

Note 1: Poisson ratio depends only slightly on porosity.

From Z. Zivcova et al., Elastic properties of porous oxide ceramics, J. Europ. Ceram. Soc. (2009)

Effective elastic properties for materials involving damage progression

From micro scale to macro scale (influence of microcracks)

➢ At macroscopic level (Damaged Material):

Apparent stress: $\sigma^* = \frac{F}{A}$

Apparent Young's modulus: $E^* = \frac{\sigma^*}{\varepsilon}$

➢ At microscopic level (Local Undamaged Area):

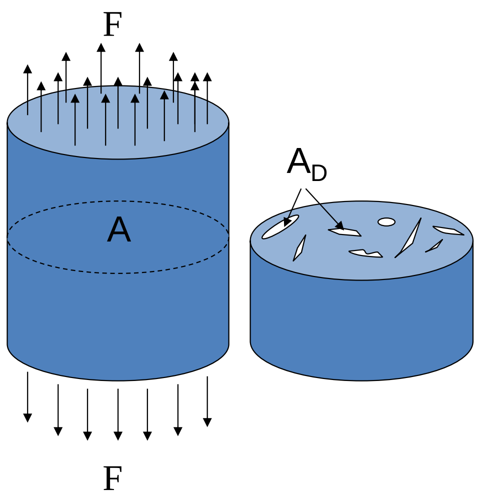

Kachanov damage parameter $D = \frac{A_D}{A}$

Real local stress: $\sigma = \frac{F}{(A - A_D)} = \frac{\frac{F}{A}}{(1 - \frac{A_D}{A})} = \frac{\sigma^*}{(1-D)}$

$$[D] = \begin{bmatrix} D_1 & D_4 & D_5 \\ D_4 & D_2 & D_6 \\ D_5 & D_6 & D_3 \end{bmatrix}$$

D could also be a tensor

Real local Young's modulus: $E_0 = \frac{\sigma}{\varepsilon}$

➔Finally, apparent Young's modulus of Damaged Material:

$$E^* = \frac{\sigma.(1-D)}{\varepsilon} = E_0.(1-D)$$

Note : Damaged material could be regarded as a material with the modulus reduced by factor (1 – D)

Modelling (FEM) of damage progression during loading

- **Application of a tensile load**

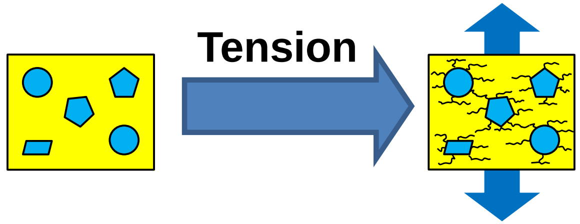

- **3 scales should be considered :**
  - **Very locally ➔ no damage**
  - **Around inclusions ➔ large damage**
  - **Macroscopic level ➔ averaged damage**

- **Stress versus strain**

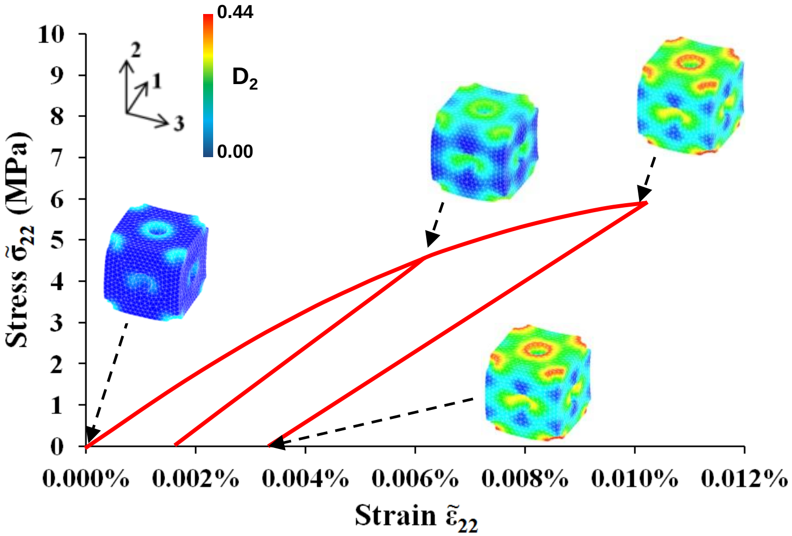

- Averaged Kachanov parameter D_2 versus strain

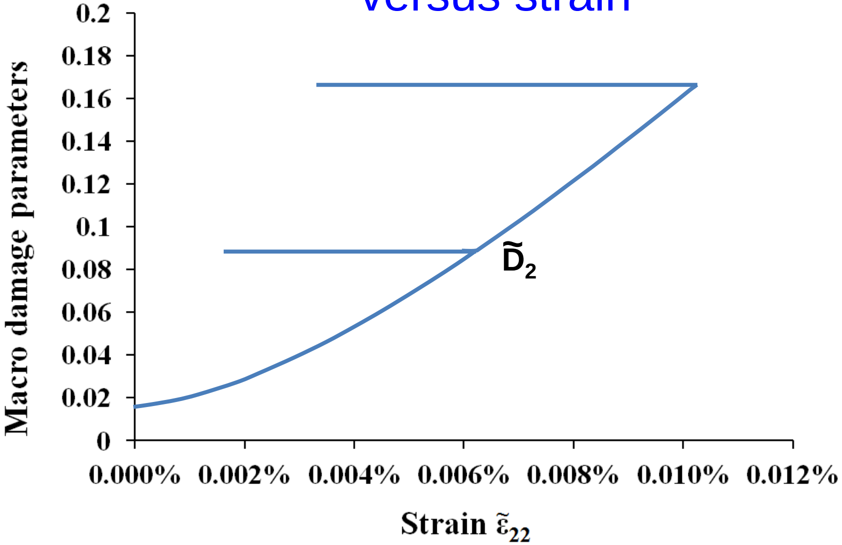

From R.Grasset-Bourdel, PhD, Leoben-Limoges (2011)

Influence of temperature on elastic properties at very local scale

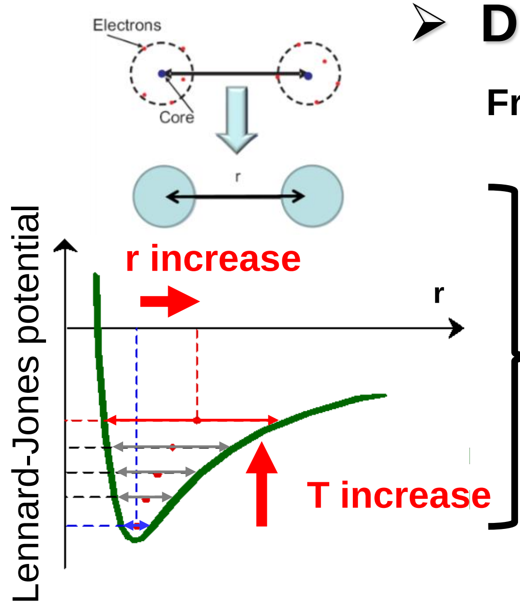

➔ **Stiffness decrease**

➢ Decrease of K (bulk modulus) versus temperature

From classical thermodynamics

$$K = K_o . \exp\left(- \int_{T=0}^{T} \alpha_V(T) . \delta_V(T) . dT \right)$$

$\alpha_V(T)$: volume thermal expansion

$\delta_V(T)$: Anderson-Grüneisen parameter

From J. Garai, "Temperature dependence of the isothermal bulk modulus", J. Appl. Phys. (2007)

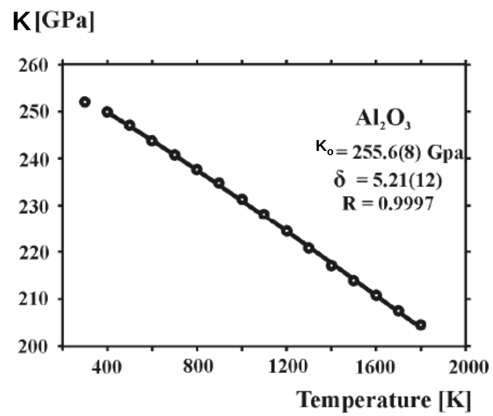

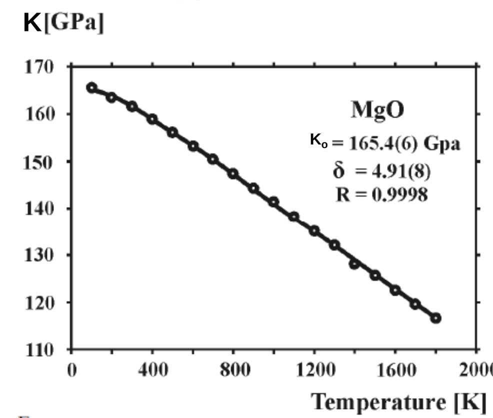

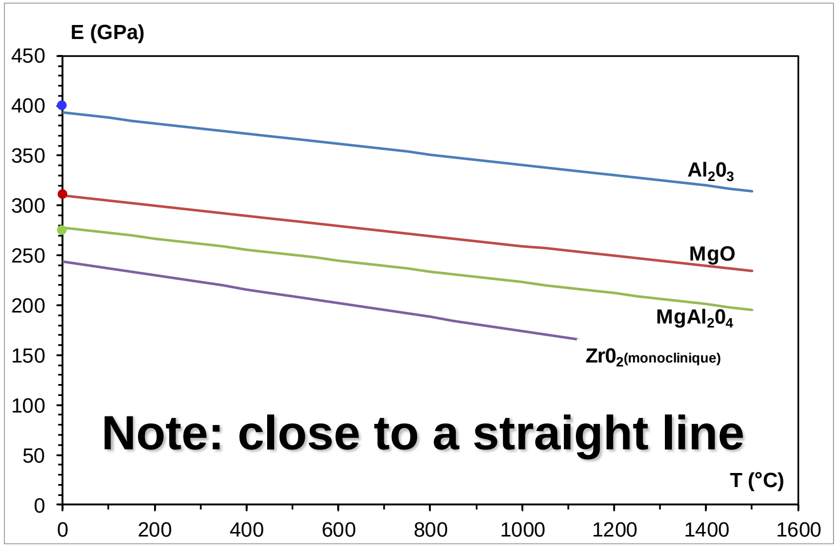

Note: close to a straight line

➔ Empirical relation first proposed for E

$$E = E_o - b.T.\exp(-T_o / T)$$

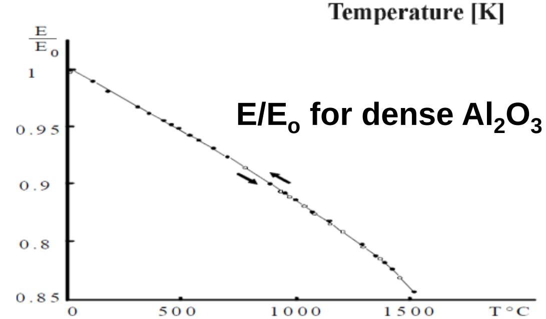

From J.B.Jr. Wachtman et al., "Exponential temperature dependance of Young's modulus for several oxides", Phys. Rev., (1961)

Understanding microstructure effects in model materials: in case of debonding between aggregates and matrix

Effect of thermal expansion mismatch between aggregates and matrix

$\alpha_m - \alpha_p < 0$

$\alpha_m = 4.6\ 10^{-6}\ K^{-1}$

$\alpha_p = 7.6\ 10^{-6}\ K^{-1}$

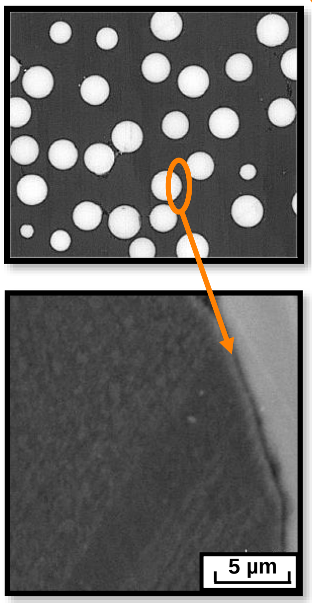

Damaged

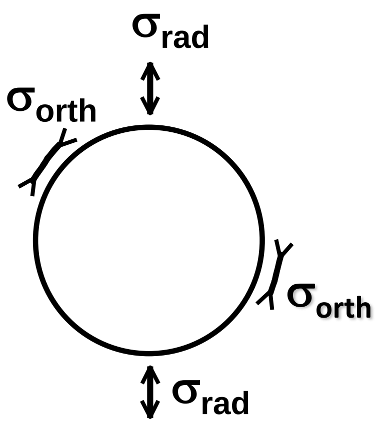

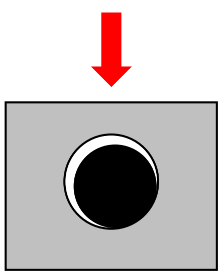

Decohesive interfaces (at 20° C)

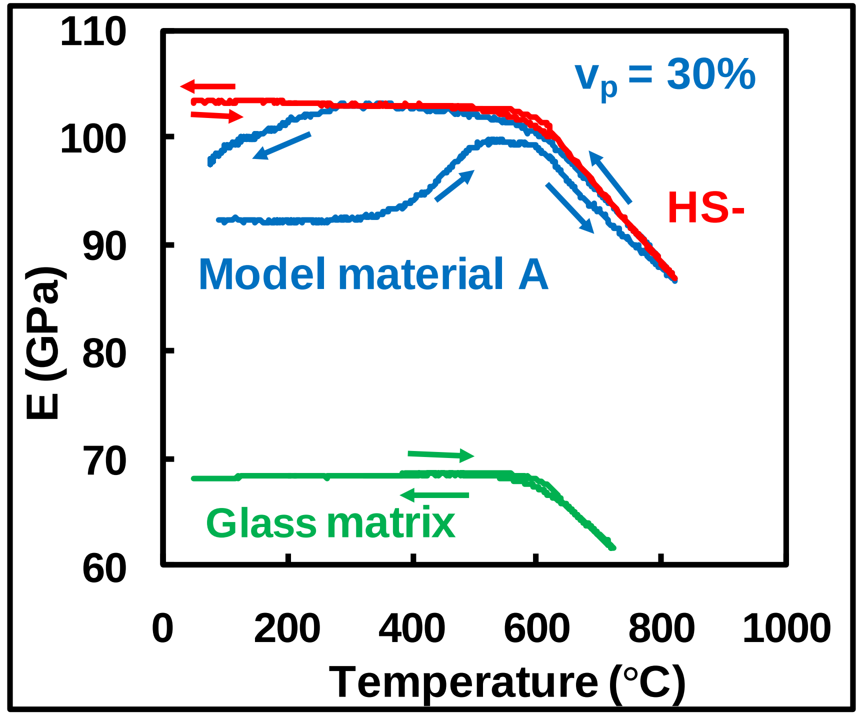

Note 1: Glass transition induce change in slope

Note 2: Good estimation by HS- at high temperature

Note 3: Debonding ➔ low value of E at 20° C

Note 4: Cracks closure ➔ E increases during heating

Note 5: Cracks open ➔ E decreases during cooling

From N. Tessier-Doyen, PhD, Limoges, (2003)

Understanding microstructure effects in model materials: in case of microcracking in the vicinity aggregates

Effect of thermal expansion mismatch between aggregates and matrix

$\alpha_m - \alpha_p > 0$

$\alpha_m = 11.6\ 10^{-6}\ K^{-1}$

$\alpha_p = 7.6\ 10^{-6}\ K^{-1}$

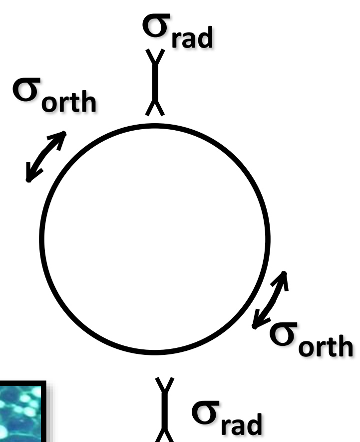

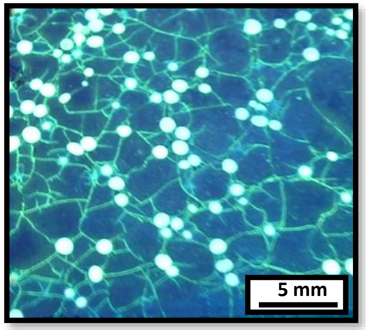

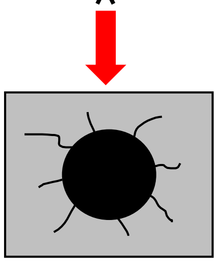

Damaged

Microcracked matrix

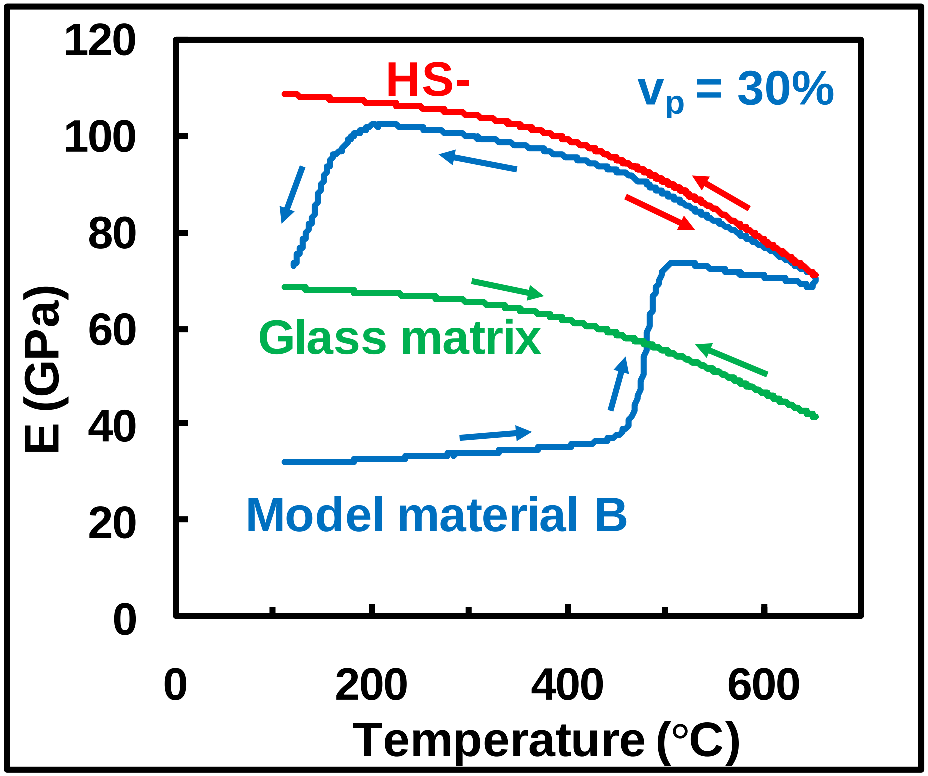

Note 1: Good estimation by HS- at high temperature

Note 2: Microcraks➔ very low value of E at 20° C

Note 3: Cracks closure ➔ E increases during heating

Note 4: Cracks open ➔ E decreases during cooling

From N. Tessier-Doyen, PhD, Limoges, (2003)

Understanding microstructure effects in real materials: case of cordierite-mullite

Refractory plate used for roof tiles production

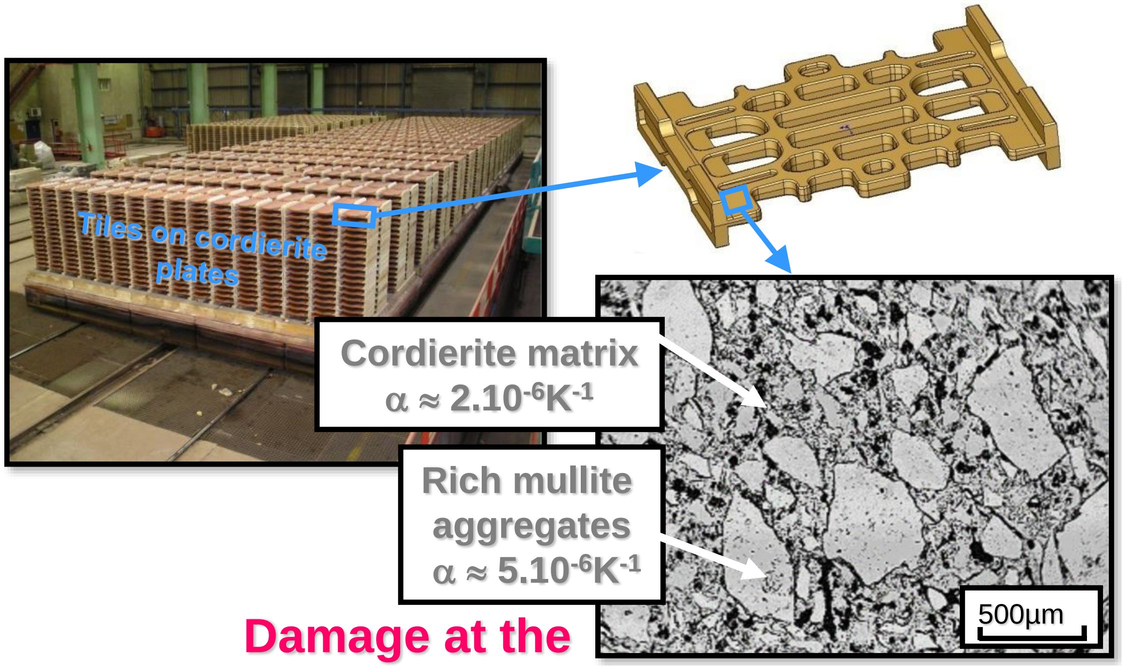

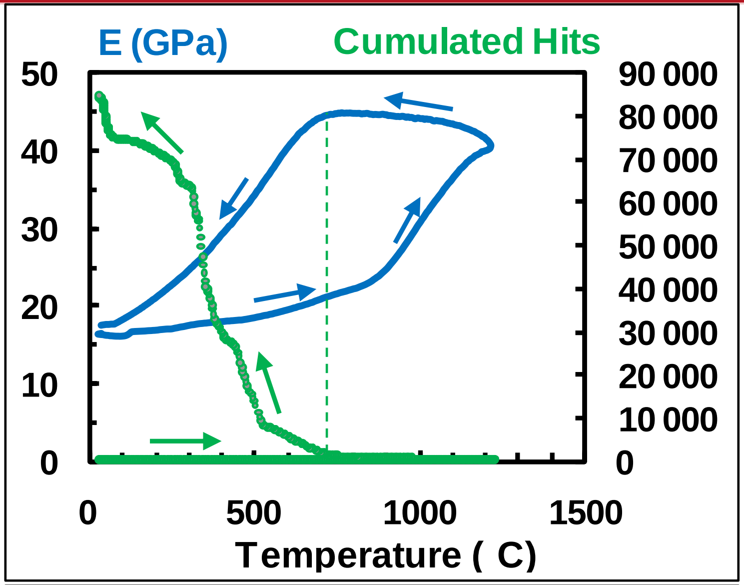

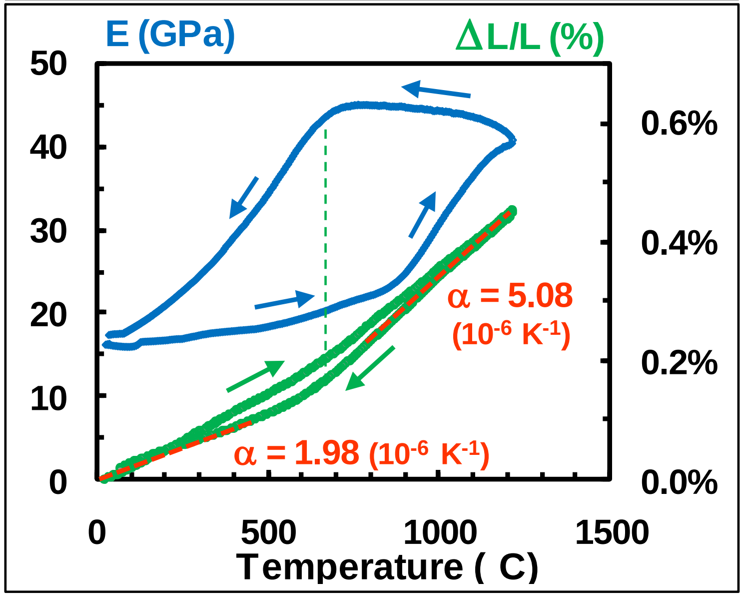

Damage at the interface between aggregates and matrix

- ➢**Hysteresis effect on E versus T**
- ➢**Acoustic emission during cooling**
- ➢**Change of slope in dilatometry**

From a study for Terreal, Limoges, (2006)

Understanding microstructure effects in real materials: case of magnesia-spinel

Refractory brick used for cement production

Cement rotary kiln

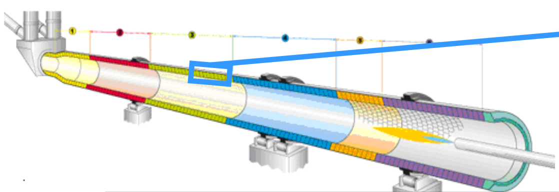

Magnesia matrix
Open porosity : 18.6%-24.5%
α_{MgO} = 13.3 $*10^{-6}$ K^{-1}

Spinel inclusion
Close porosity : 6.8%
α_{spinel} = 8.9 $*10^{-6}$ K^{-1}

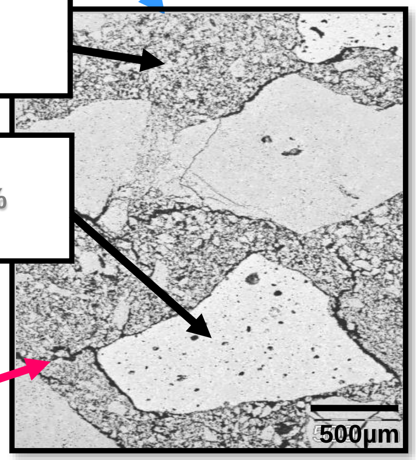

Microcracked matrix Arround the aggregates

- ➢Rather low value of E at 20° C (far from HS-)
- ➢Hysteresis effect on E versus T
- ➢E becomes closer to HS- when heating

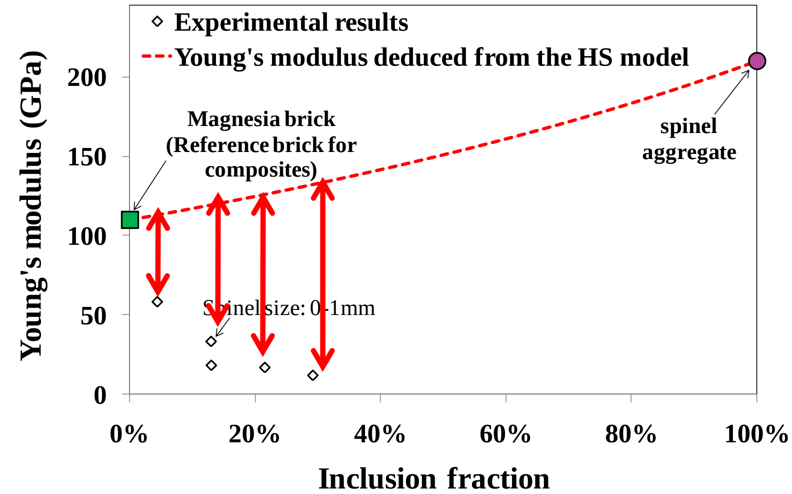

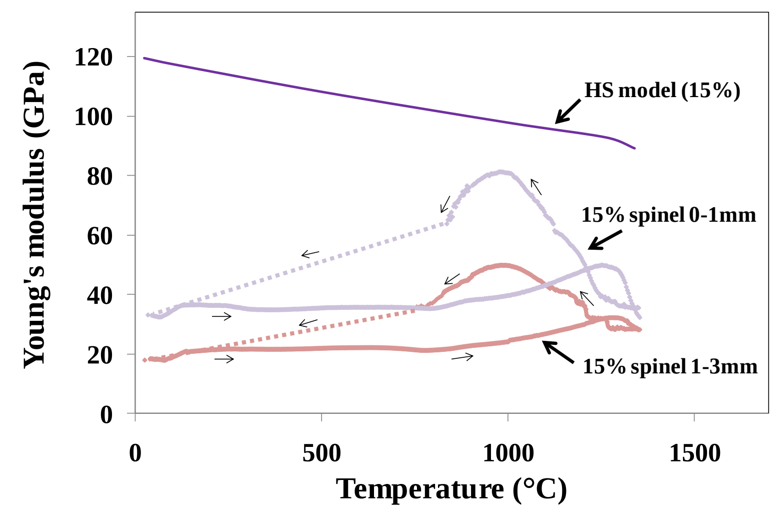

From R. Grasset-Bourdel, PhD, Leoben/Limoges, (2011)

Understanding microstructure effects in real materials: case of alumina-carbon

Refractory tubes for steel continuous casting

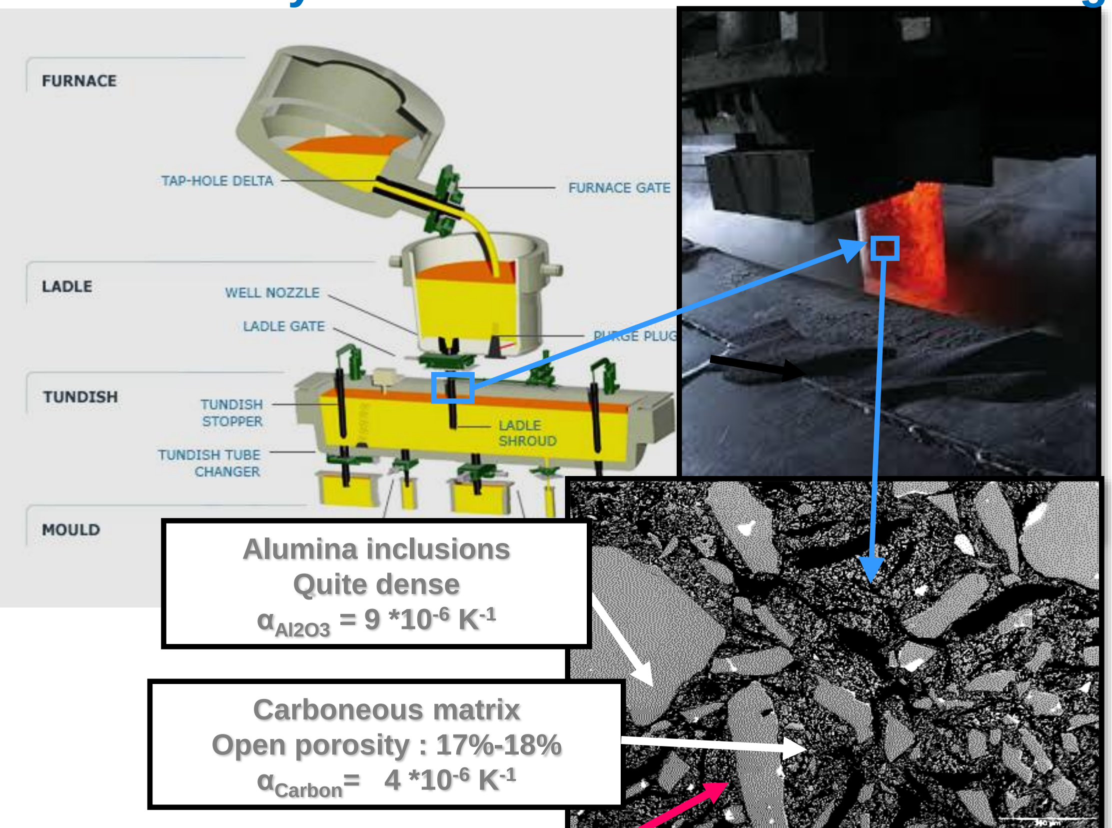

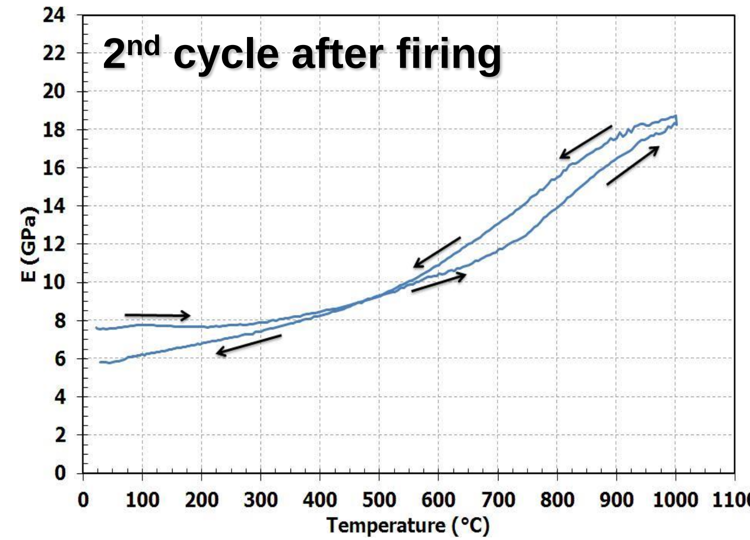

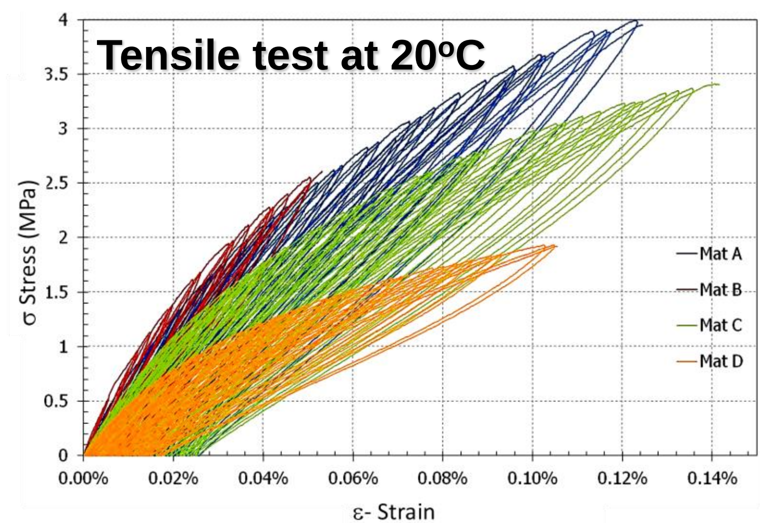

From D. Dupuy, PhD, Limoges, (2015)

Decohesive interface around the inclusions

- **Very low value of E at 20°C (far from HS-)**
- **E increase toward HS- when heating**
- **Rather no hysteresis effect on E versus T**
- **Large non linear Stress-Strain behaviour (influence of μstructure)**

Understanding microstructure effects in real materials: case metallic antioxidant addition on alumina-carbon

Refractory tubes for steel continuous casting

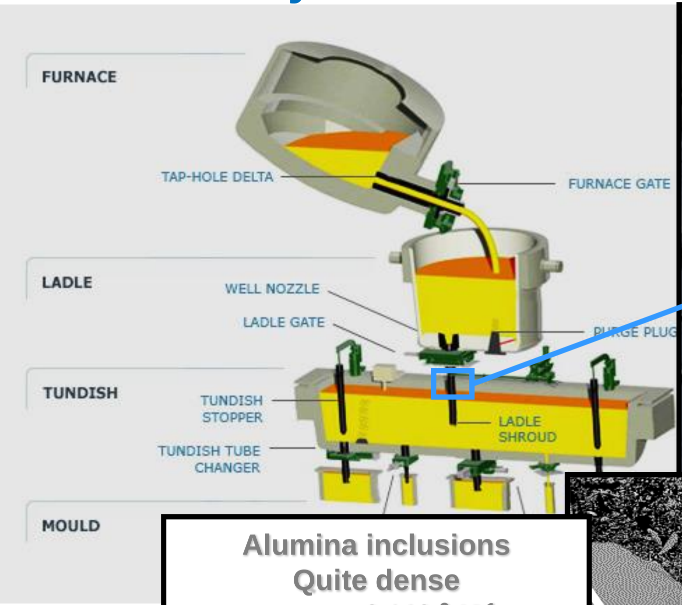

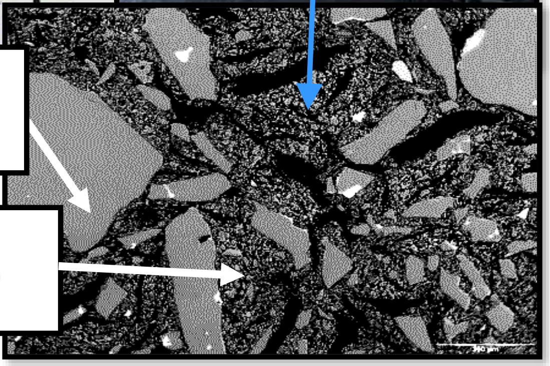

Alumina inclusions
Quite dense
$\alpha_{Al2O3} = 9 * 10^{-6} K^{-1}$

Carboneous matrix
Open porosity : 17%-18%
$\alpha_{Carbon} = 4 * 10^{-6} K^{-1}$

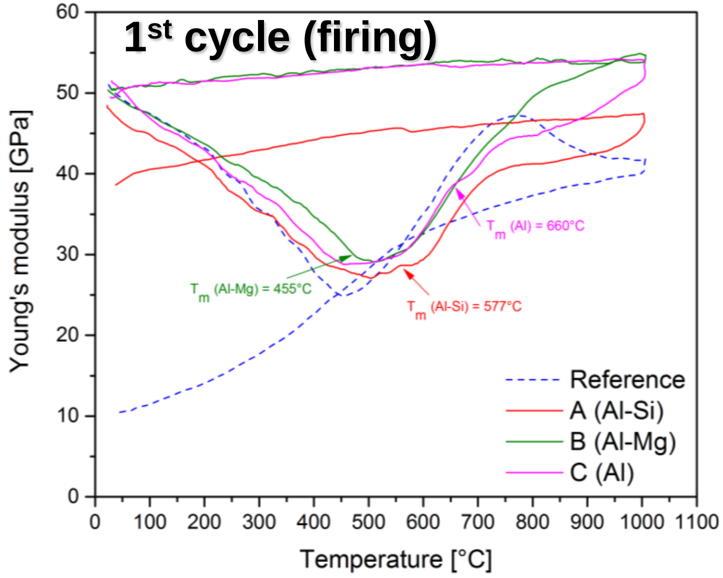

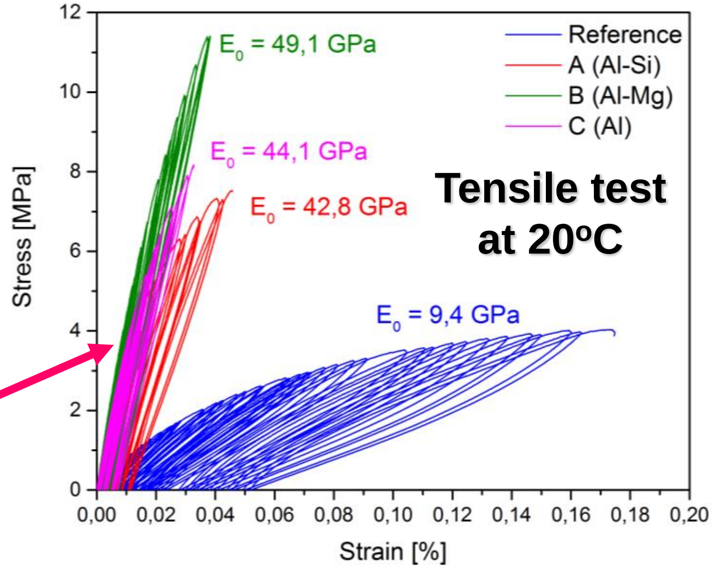

Only 2.5% of metallic antioxidant addition significantly rigidify the refractory

From A. Warchal, PhD, Limoges, (to come 2019)

Thermal expansion from crystal symmetry, few examples

- **Increase of interatomic distances versus temperature**

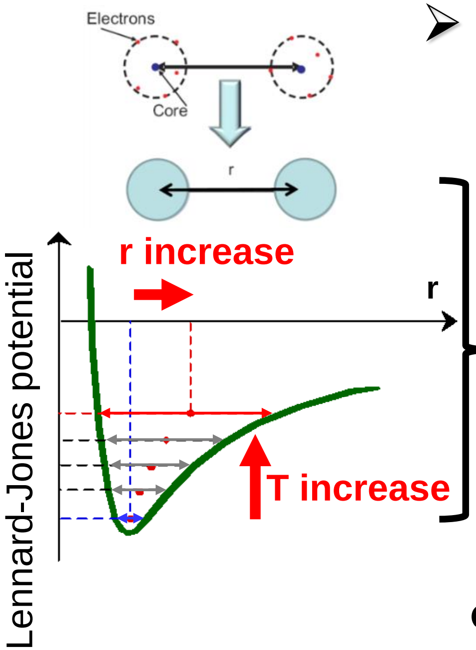

→distance increase

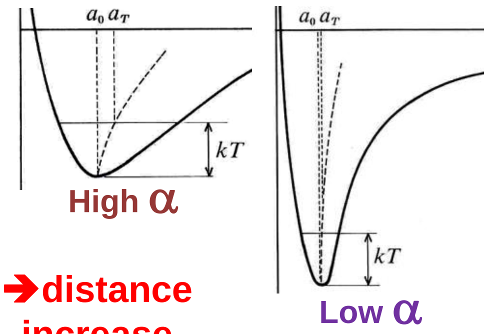

$$\alpha(T) = \frac{\Delta r}{r}\Big|_T$$

$$\alpha(T) = a_0 + a_1.T + a_2.T^{-2}$$

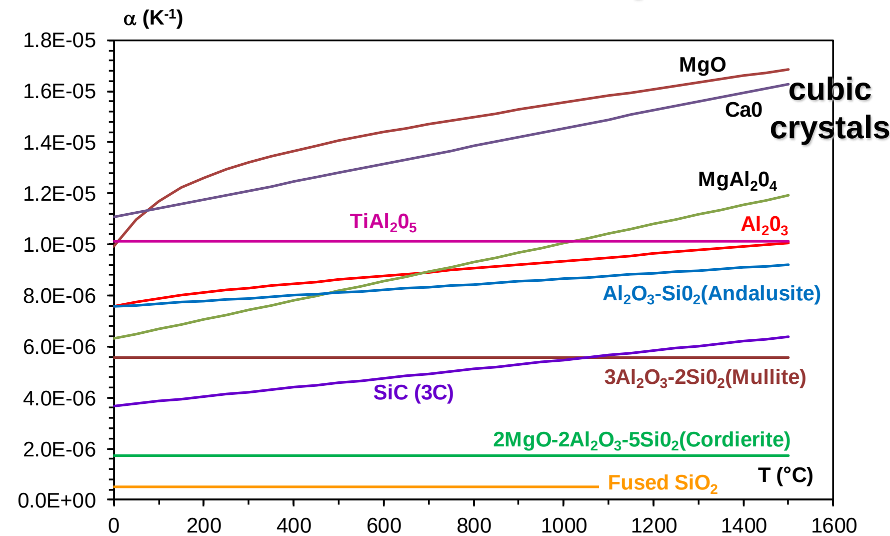

- **Non cubic crystals → anisotropy**

Ex: orthorhombic

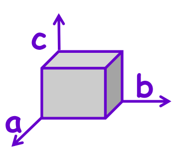

	α (10^{-6}.K^{-1})		
Axis	α_a	α_b	α_c
Al_2SiO_5	12.5	8.05	2.33
$Al_6Si_2O_{13}$	3.9	7	5.8
$Mg_2Al_4Si_5O_{18}$	3.87	2.58	-1.29
$TiAl_2O_5$	-2.38	11.97	20.80

From Y. Fei, "Thermal Expansion", *Handbook, (1995)*

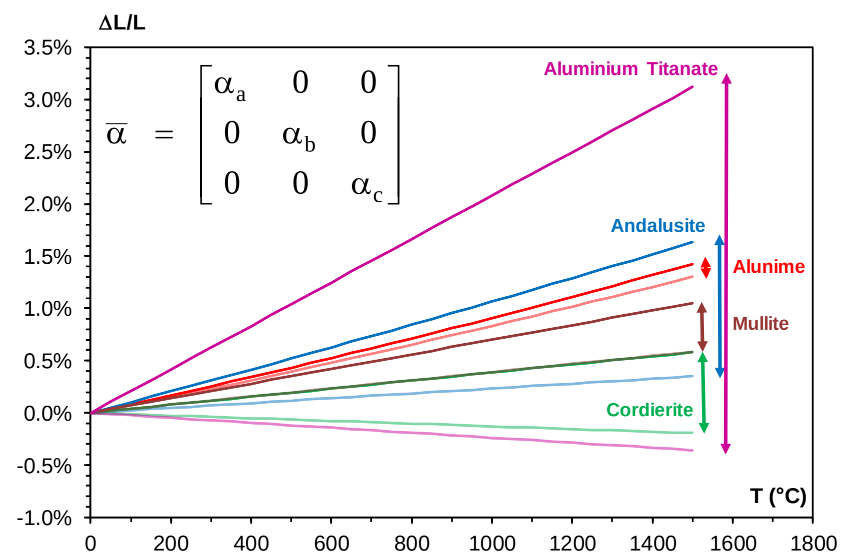

$$\bar{\alpha} = \begin{bmatrix} \alpha_a & 0 & 0 \\ 0 & \alpha_b & 0 \\ 0 & 0 & \alpha_c \end{bmatrix}$$

Effect of thermal expansion anisotropy: case of polycrystalline Alumina

- **Influence of grain size**

$$\overline{\alpha}\,(10^{-6}\,K^{-1}) = \begin{bmatrix} 8.62 & 0 & 0 \\ 0 & 8.62 & 0 \\ 0 & 0 & 9.38 \end{bmatrix}$$

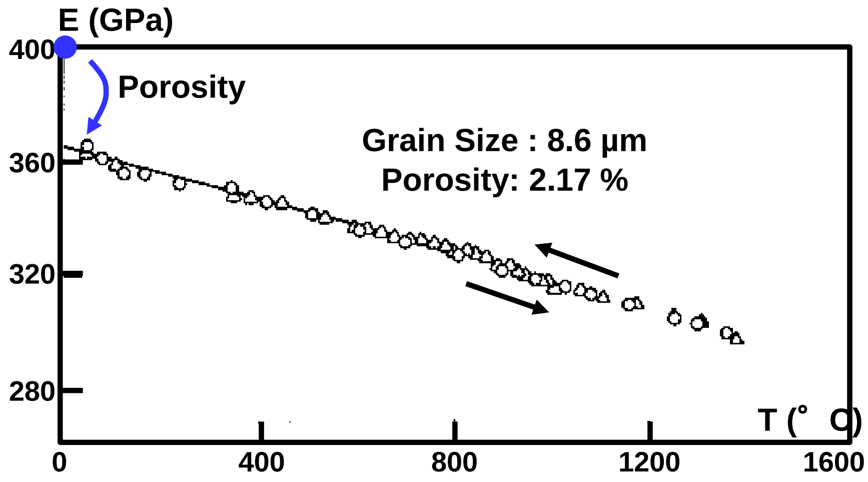

➔ Critical size of about 60-70µm

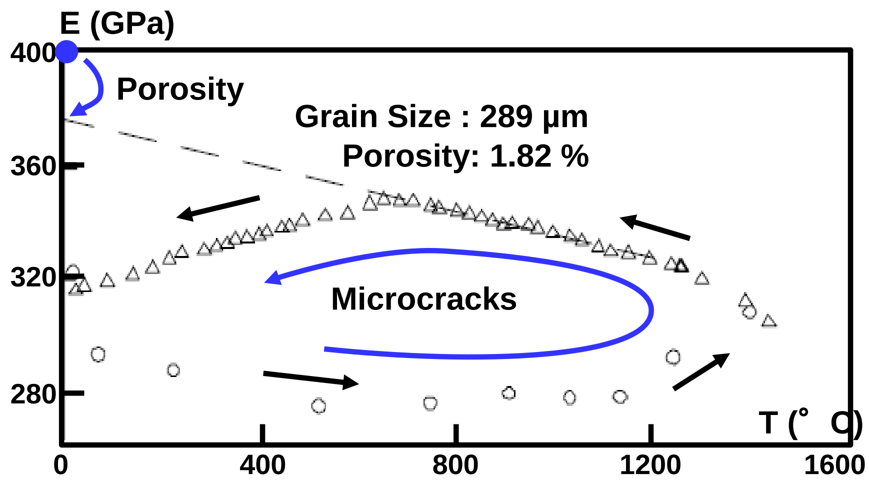

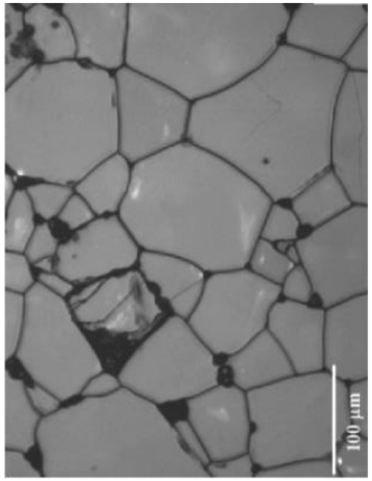

From E.D. Case et al., "Microcracking in large-grain Al_2O_3", Materials Science and Engineering, (1981)
From S.G. Yousef et al., "Microcrack Evolution in Alumina Ceramics", J. Am. Ceram. Soc., *(2005)*

Effect of thermal expansion anisotropy: case of polycrystalline Aluminium titanate

➢ Influence of grain size

$$\overline{\alpha}\,(10^{-6}K^{-1}) = \begin{bmatrix} -2.38 & 0 & 0 \\ 0 & 11.97 & 0 \\ 0 & 0 & 20.80 \end{bmatrix}$$

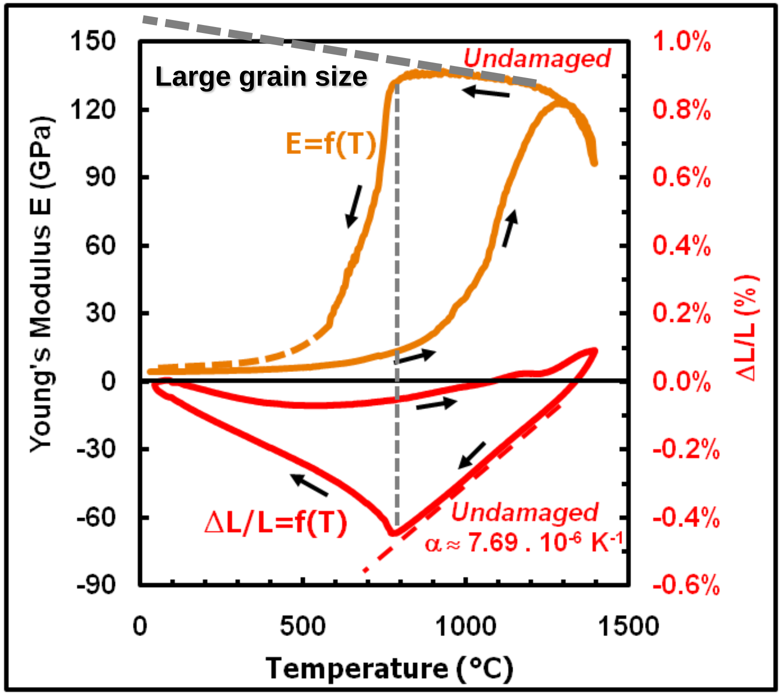

➔ Critical size of about 1µm

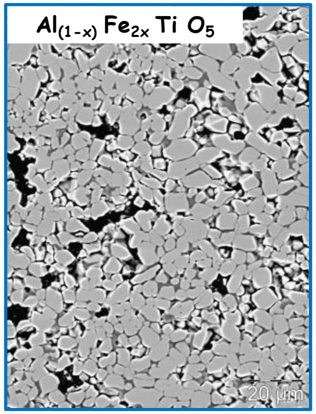

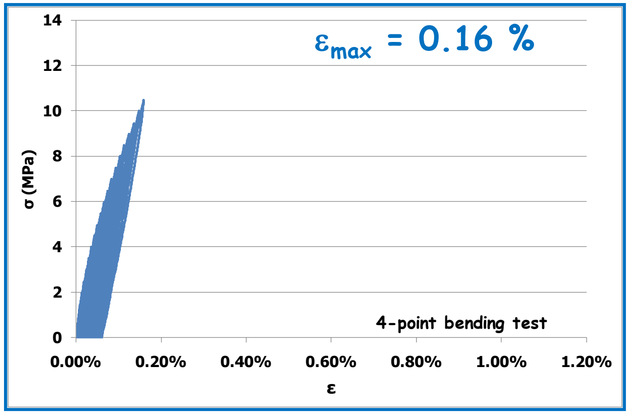

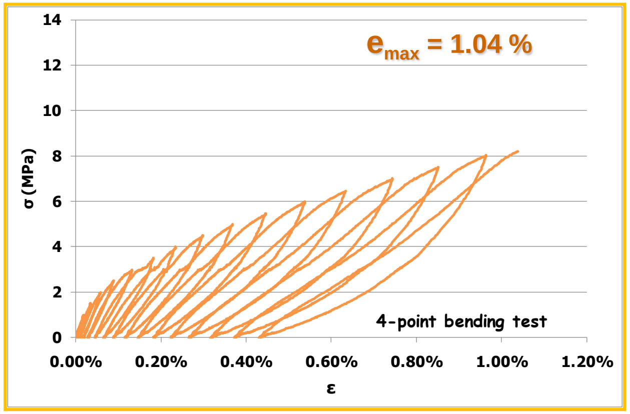

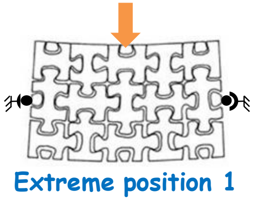

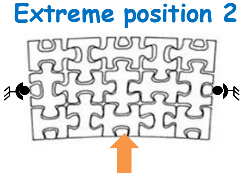

➔ Promote flexibility (high strain to rupture)

From A.Gallet-Doncieux, "Flexibility of Aluminium Titanate", Limoges (2010)

Effect of thermal expansion anisotropy: case of Andalusite based castables

➢ Influence of CTE mismatch between aggregates and matrix

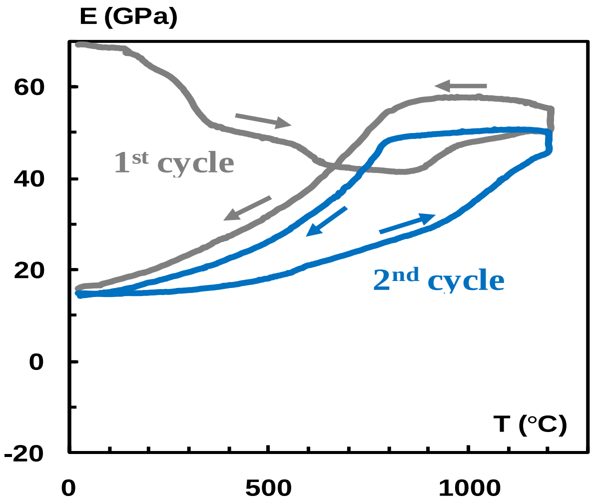

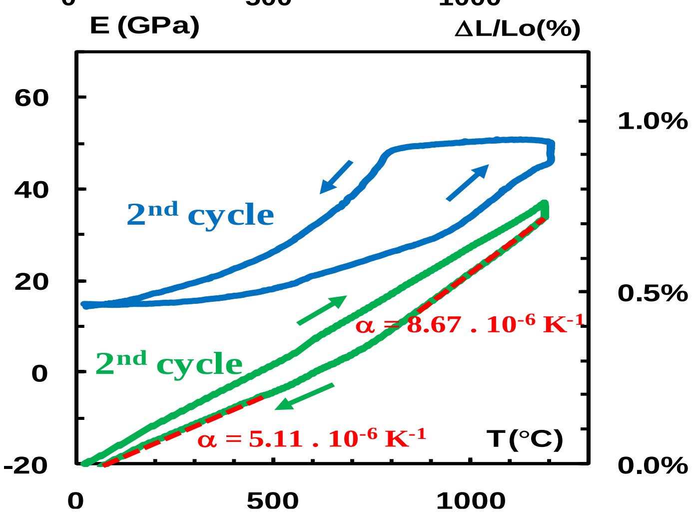

Cementitous matrix

$$\alpha\,(10^{-6}\,\mathrm{K}^{-1}) = 7.6$$

Andalusite aggregates

$$\overline{\alpha}\,(10^{-6}\,\mathrm{K}^{-1}) = \begin{bmatrix} 12.9 & 0 & 0 \\ 0 & 9.6 & 0 \\ 0 & 0 & 3.1 \end{bmatrix}$$

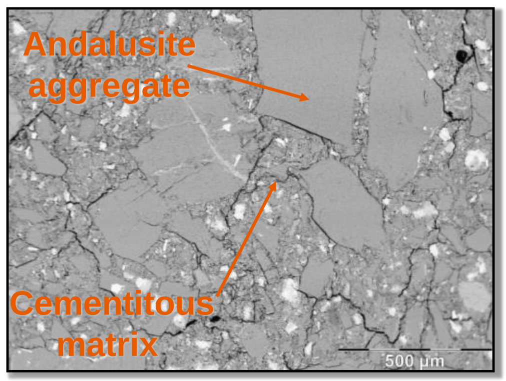

➔ Damage can promote flexibility

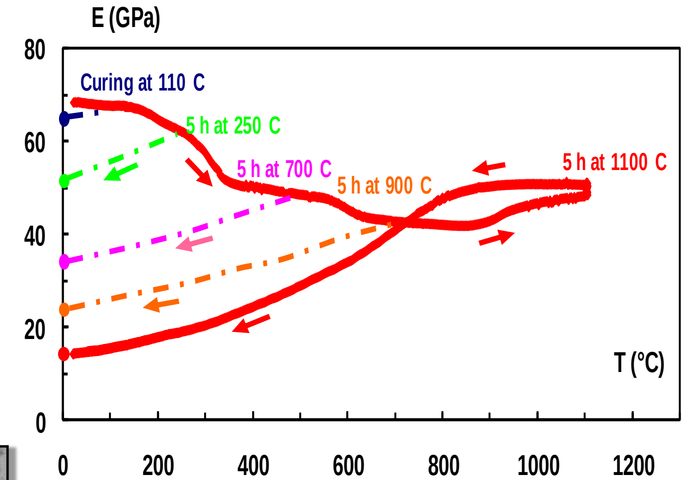

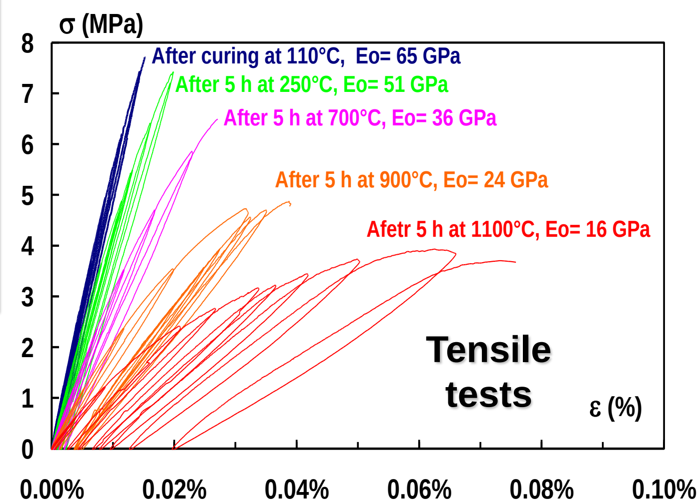

From Mahdi Kakroudi., PhD, Limoges (2007)

Effect of thermal expansion mismatch: case of magnesia-spinel refractories

➢ **Thermal damage during process**

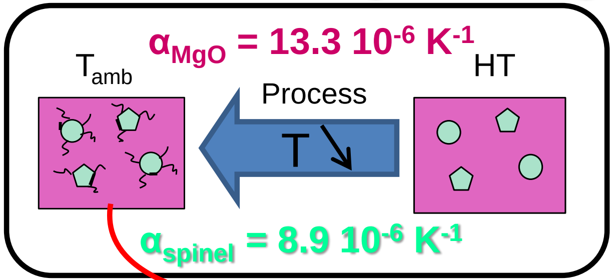

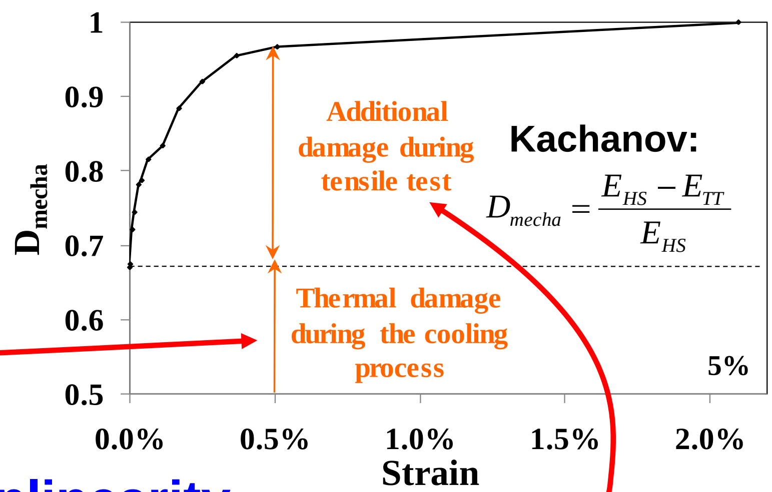

➔Spinel aggregates increases the nonlinearity

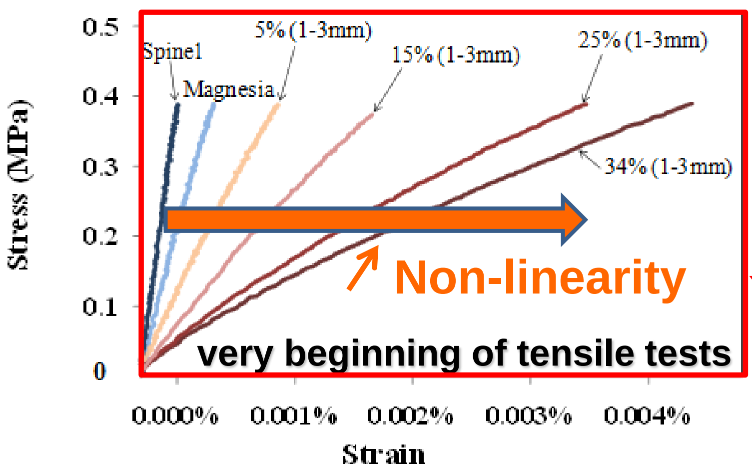

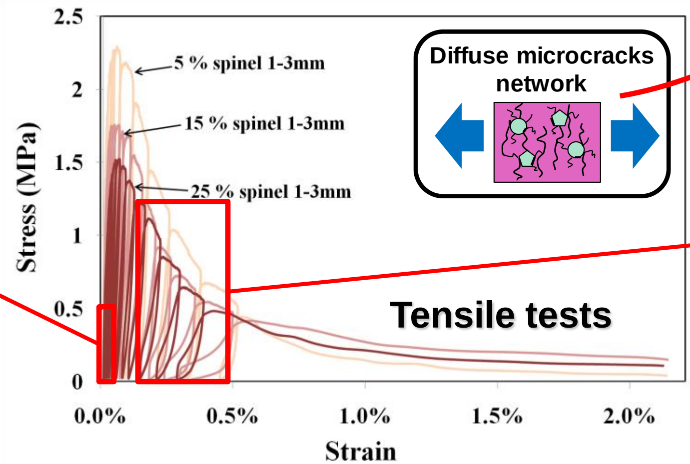

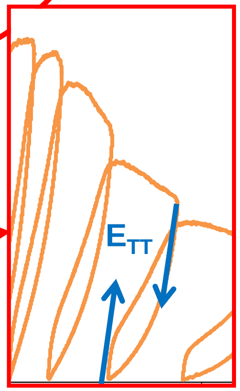

➔ **Promote flexibility (high strain to rupture)**

➔ **Reduce brittleness**

From R.Grasset-Bourdel, PhD, Leoben-Limoges (2011)

Effect of thermal expansion mismatch: effect of hercinyte addition on magnesia-spinel refractories

Application of 2P-DIC during Wedge Splitting

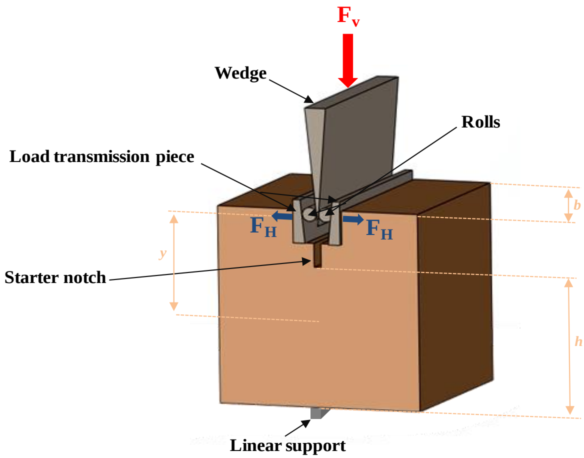

Magnesia (MgO) matrix : α = 10-17 *10^{-6} K^{-1}

Spinel ($MgAl_2O_4$) inclusions: α = 6-12 *10^{-6} K^{-1}

Hercynite ($FeAl_2O_4$) inclusions: α = 5-15 *10^{-6} K^{-1}

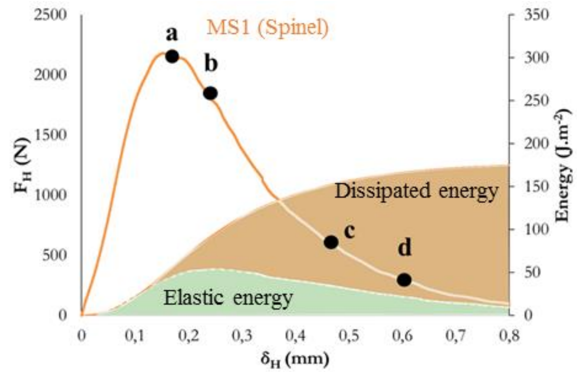

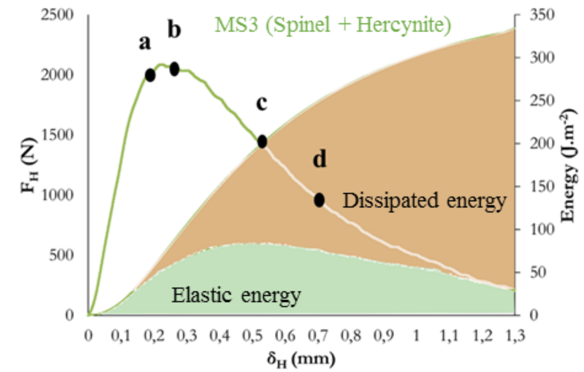

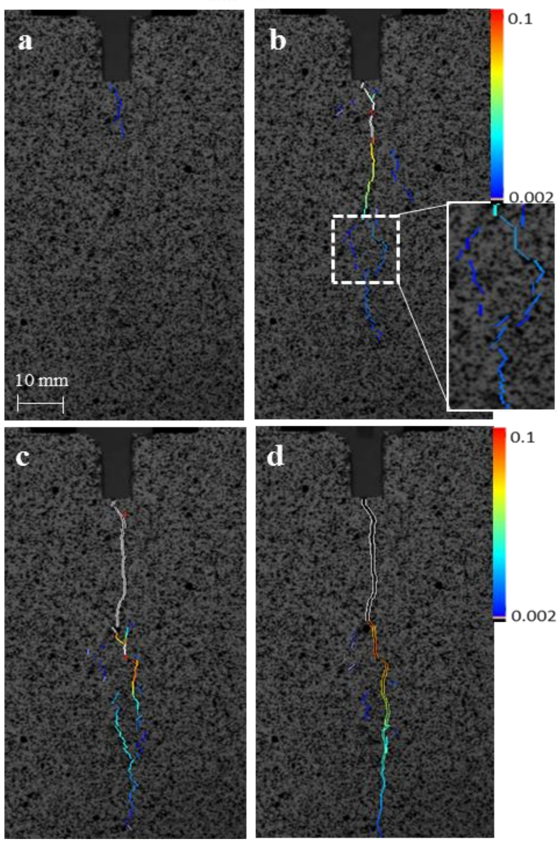

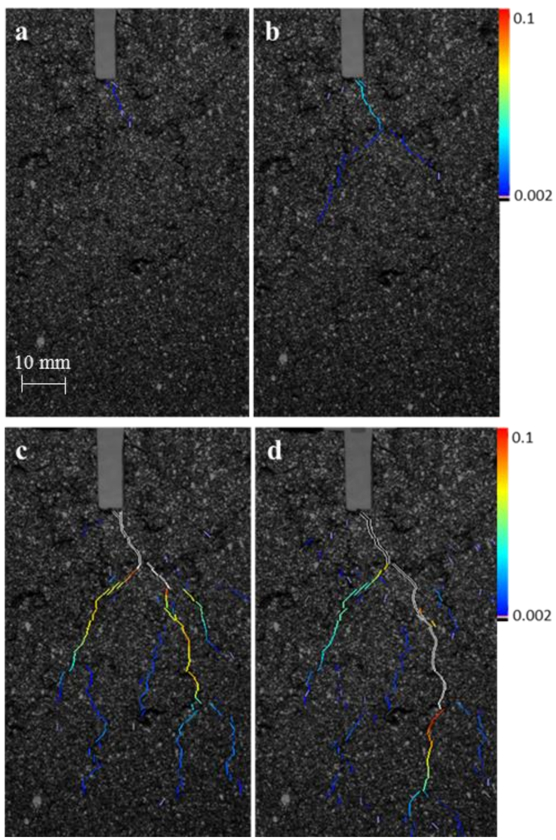

- **High dissipated energy**
- **Extensive crack-branching**
- **Large fracture process zone size**

From I.Khlifi, PhD, Limoges (to com 2019)

Modelling (FEM) the effect of thermal expansion mismatch in case of magnesia-spinel

➢ **Damage progression when loaded**

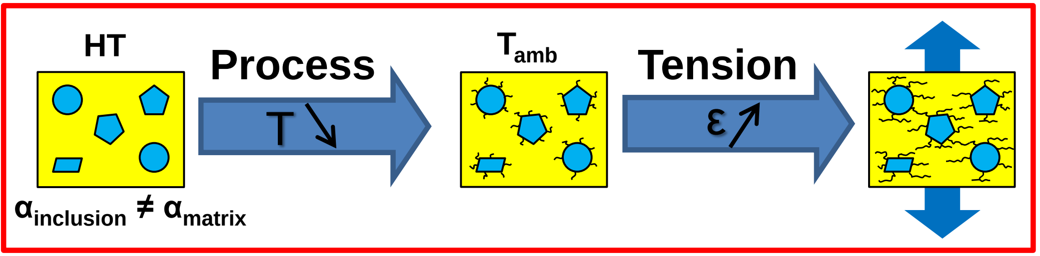

Damage state after loading

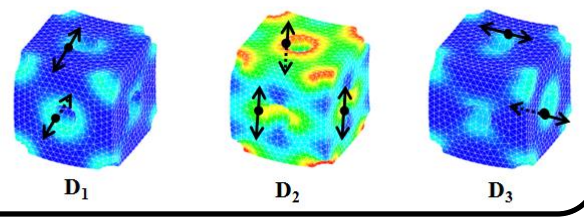

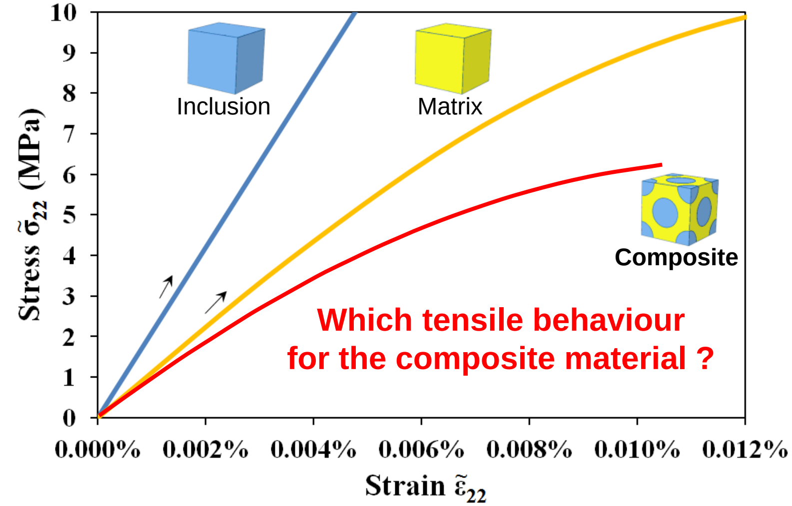

Orthotropic damage model from Code Aster with regularisation method

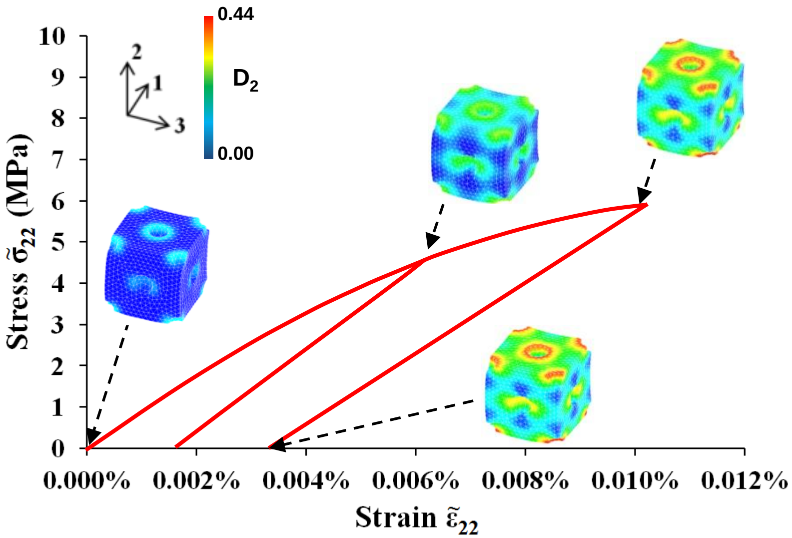

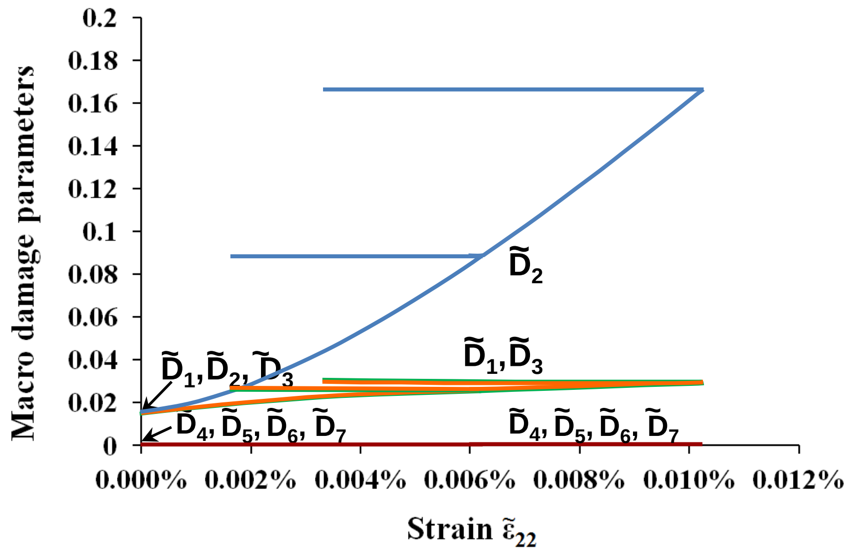

From R.Grasset-Bourdel, PhD, Leoben-Limoges (2011)

Modelling (DEM) the effect of thermal expansion mismatch in case of model material

- **Damage progression when loaded**

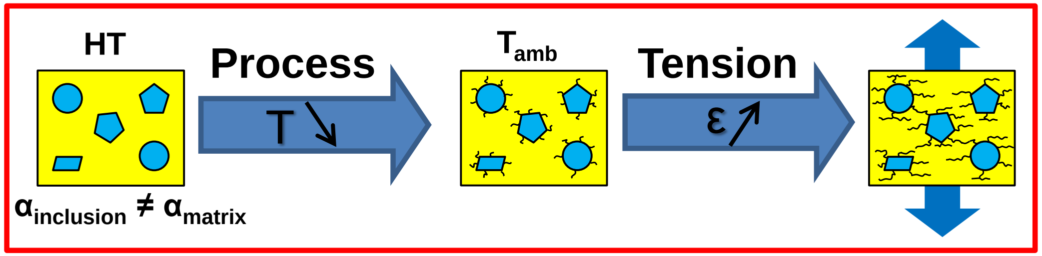

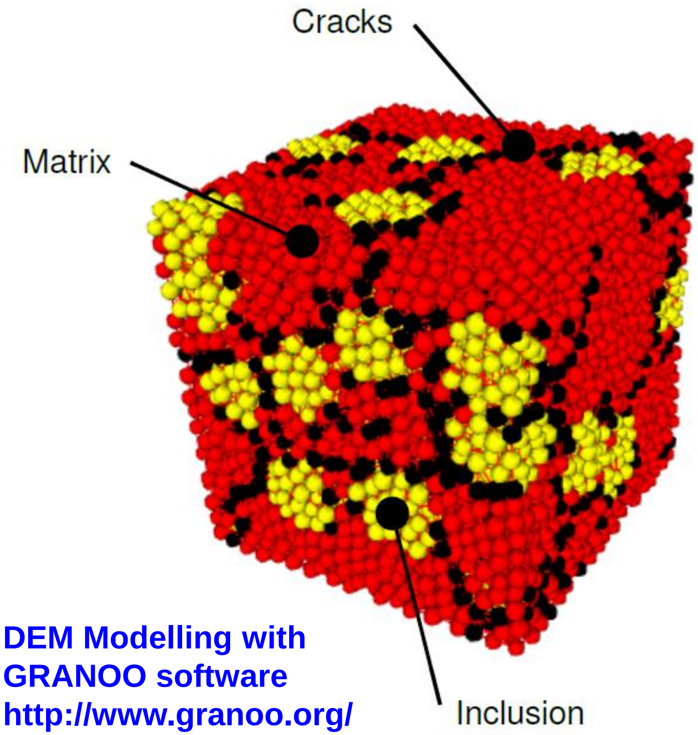

DEM Modelling with GRANOO software http://www.granoo.org/

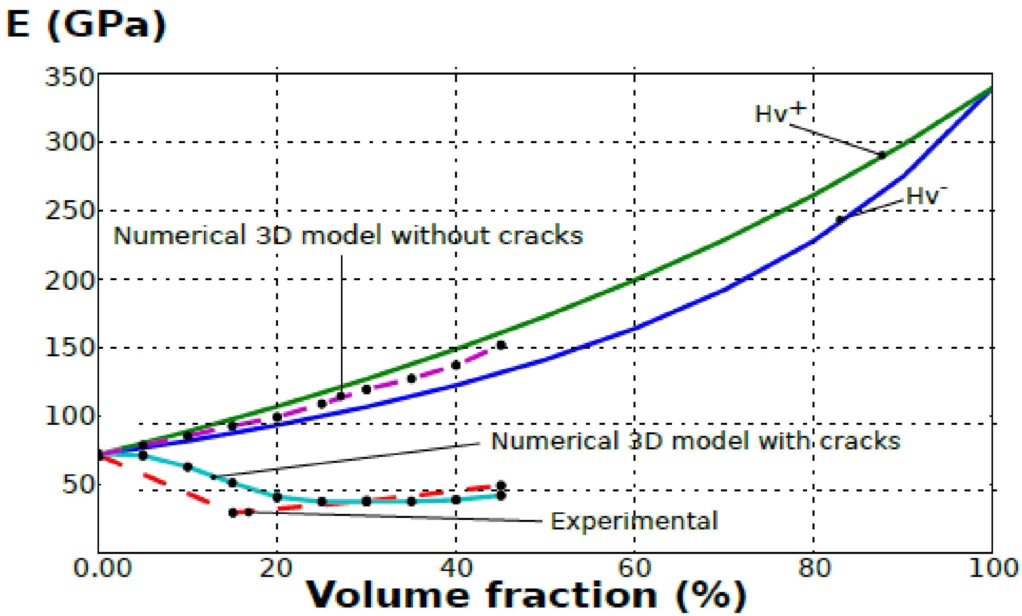

From T.T Nguyen, PhD, Limoges (to come 2019)

Conclusion and future works…

Elastic properties of heterogeneous refractory materials… **are**

- **From single crystal to poly-crystals: VRH analytical approach well suited**
- **From single phase to composites: HS analytical approach well suited**
- **Influence of porosity: Decrease could be described by exponential law**

USEFUL TO ESTIMATE VALUES

- **Damage ➔ could be quantified experimentally by differentiation from previous estimation**
- **Temperature ➔ usually a** reversible decrease (straight line)**…**
  if not, could be very useful for microstructure investigations

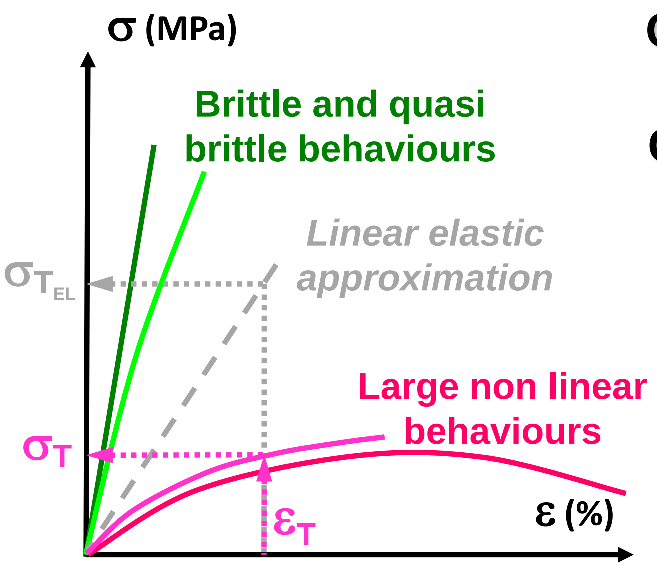

CTE MISMATCH BETWEEN CONSTITUENTS → **DIFFUSED MICROCRACKS NETWORKS**

- **Well-known decrease of E (useful with the classical thermoelastic approach)**
- **<u>Large non linear stress-strain law</u> (should absolutely be considered for thermal shocks in the case of refractories)**
- **Decrease of strength (to be limited)**
- **<u>Large increase of strain to rupture</u> (very useful in case of thermal shocks)**
- **α can also be affect**

// For their contribution to this work, a great thank…

… to industrial partners:

Vesuvius, SAINT-GOBAIN HIGH-PERFORMANCE MATERIALS, calderys REFRACTORY SOLUTIONS, IMERYS TRANSFORM TO PERFORM, TRB, Tenaris, alteo A NEW WORLD OF ALUMINA, TATA, RHI

… to university partners:

- Montanuniversität Leoben
- Nagoya Institute of Technology
- Aachen University
- Poitiers University

… to FIRE:

… to students (PhD level):

- S. PERUZZI, J-M. AUVRAY, N. TESSIER-DOYEN, E. YEUGO-FOGAING, Y. JOLIFF, M. GHASSEMI-KAKROUDI, O. BALHOUL, C. PATAPY, E. DALHEM, R. GRASSET-BOURDEL, D. DUPUY, Y. BELRHITI, F. GOURAUD, D. OHIN, A. WARCHAL, Y. LALAU, I.KHLIFI, T.NGUYEN

Université de Limoges

cnrs

SPCTS Science des Procédés Céramiques et de Traitements de Surface

UMR CNRS 7315

fiRe
Federation for International Refractory Research and Education

ATHOR
EU MSCA ETN
Refractory linings

Thank your for your attention

European Ceramic Center

Université de Limoges

cnrs

SPCTS
Science des Procédés Céramiques et de Traitements de Surface
UMR CNRS 7315

Prof. Marc HUGER
marc.huger@unilim.fr

Additional slides

Université de Limoges

CNRS

SPCTS Science des Procédés Céramiques et de Traitements de Surface
UMR CNRS 7315

Young modulus (E) measurements at high temperature

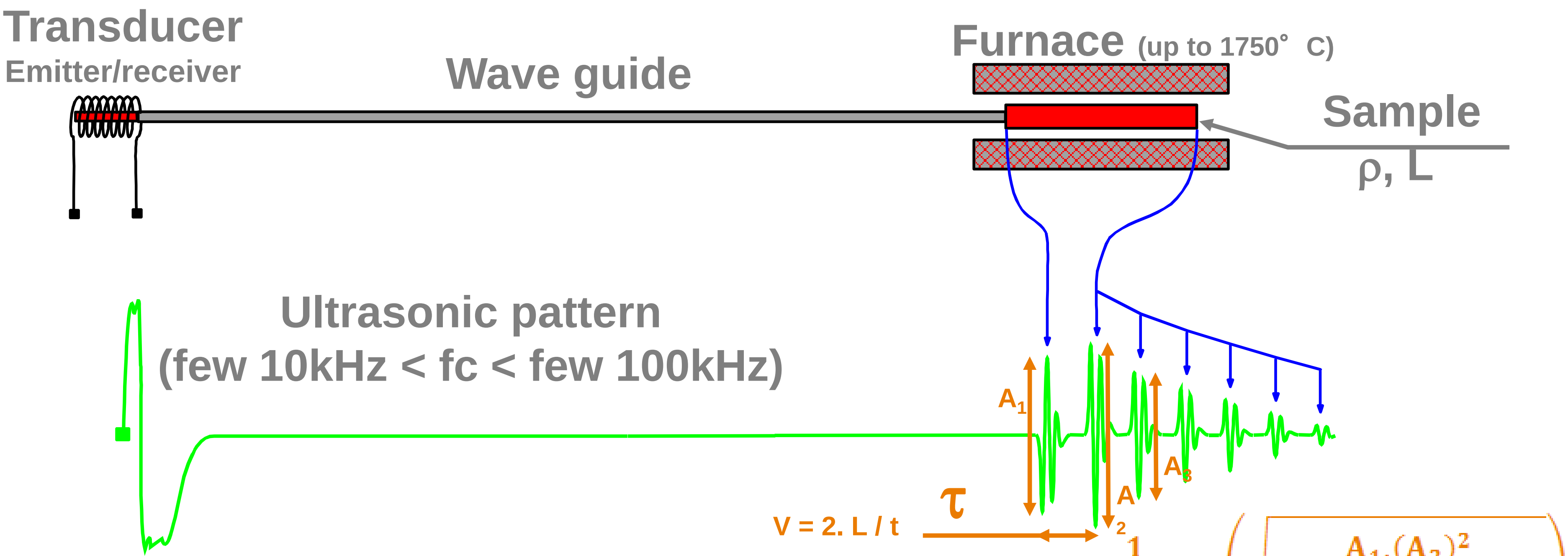

$$\alpha = \frac{1}{2.L}.\mathrm{Ln}\left(\sqrt{\frac{A_1.(A_2)^2}{A_3.((A_2)^2 + A_1.A_3)}}\right)$$

$$E_{us} = \rho \, . \, V^2$$

➔ **Study of Young's modulus variation related to microstructure evolutions versus temperature**

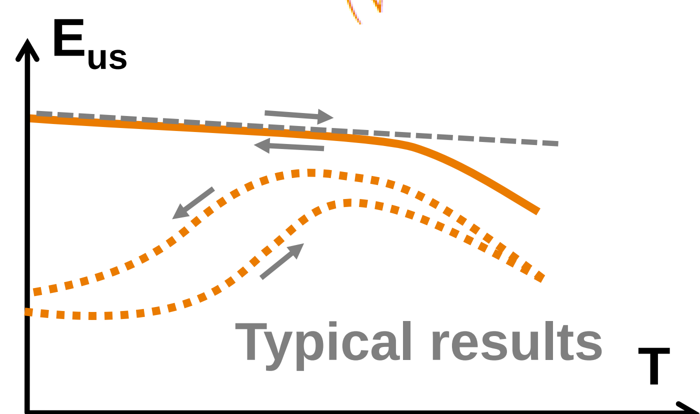

Université de Limoges

Science des Procédés Céramiques et de Traitements de Surface

UMR CNRS 7315

Acoustic emission at high temperature

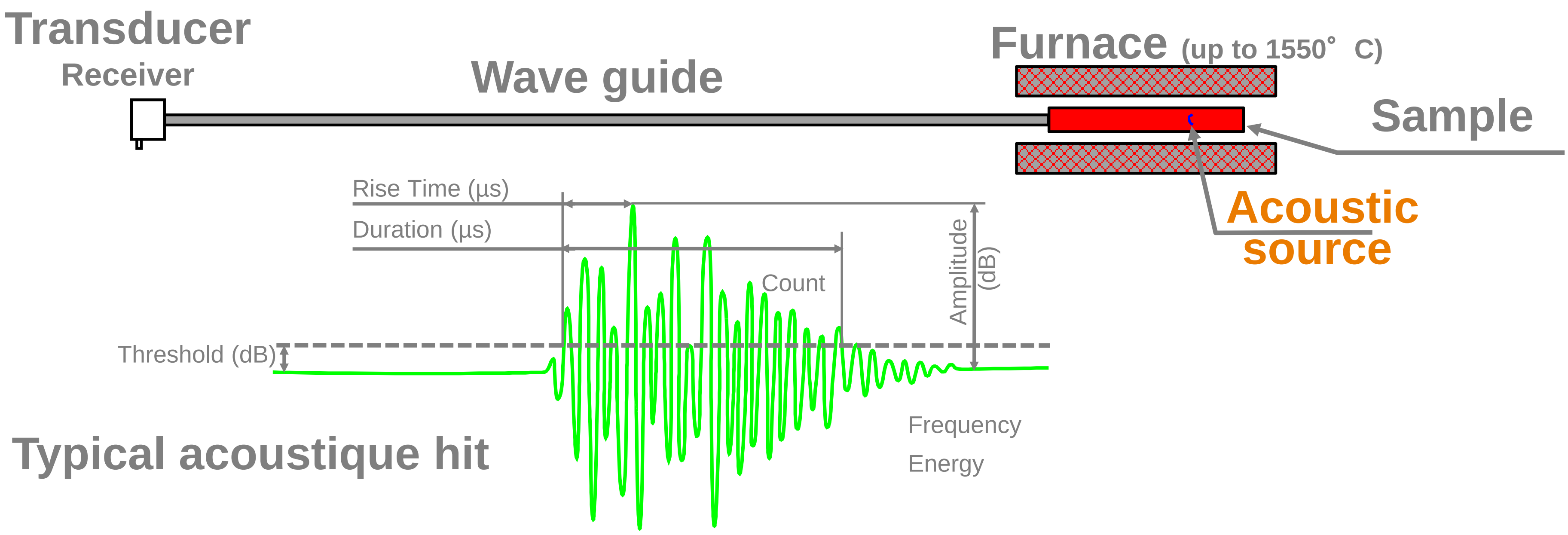

Cumulated hits

➔ Study of the chronology of damage induced by the temperature variation (indicator for the state of the microstructure)

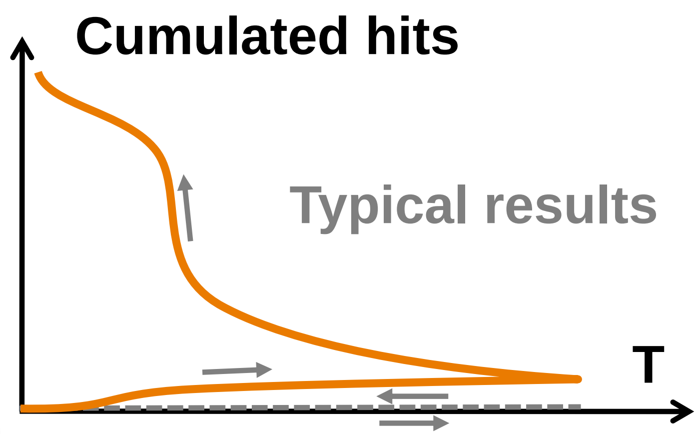

Tensile (compression) tests at high temperature

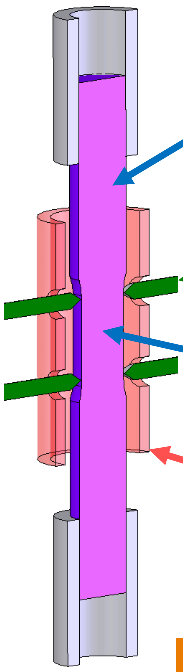

Sample : rod $\phi \approx 20$ mm, 160 to 200 mm length with steel sleeve bounded to each ends
(cylindrical machining before test)

2 Extensometers 1600 °C
(Lo = 25 mm - $\Delta L_{max} \approx 5$ µm)

Central part of the sample
Lo = 25 mm, $\phi \approx 16$ mm

Susceptor of the induction furnace

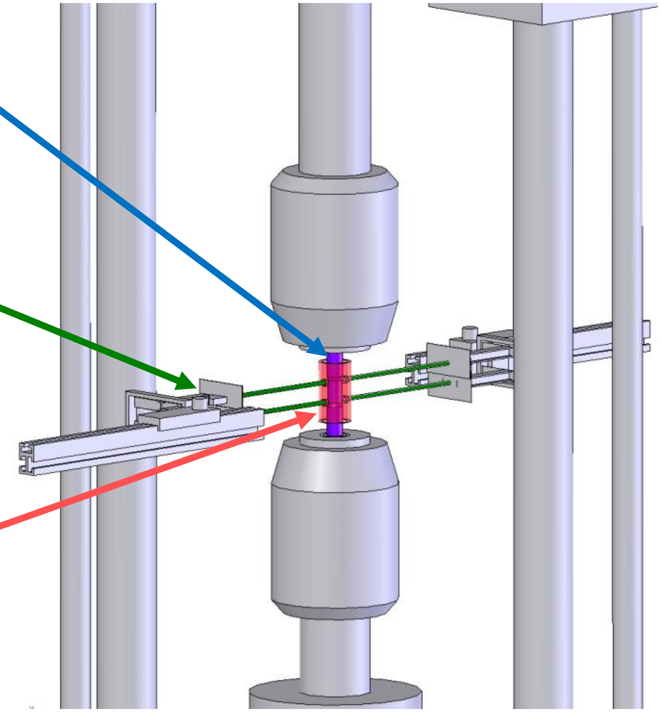

100kN Frame
Tests in the
0-5kN range

$$\sigma = f(\varepsilon)$$

➔Study of the stress-strain laws (microstructure effects) :
- **Initial Young's modulus (E_T)**
- **Non linearity (ε_r, σ_r)**

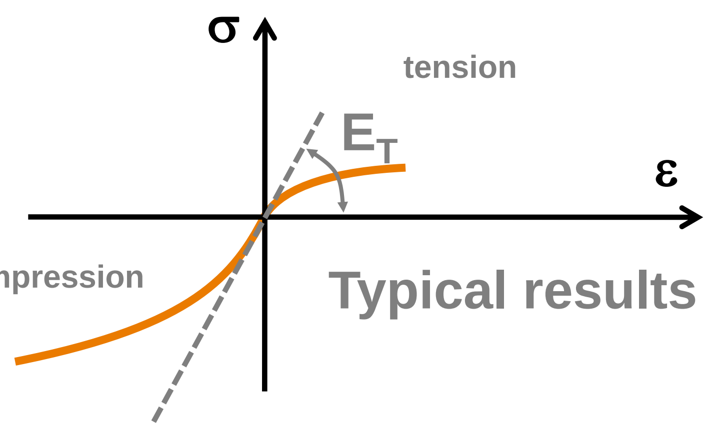

Stress-strain law, model materials versus industrial ones

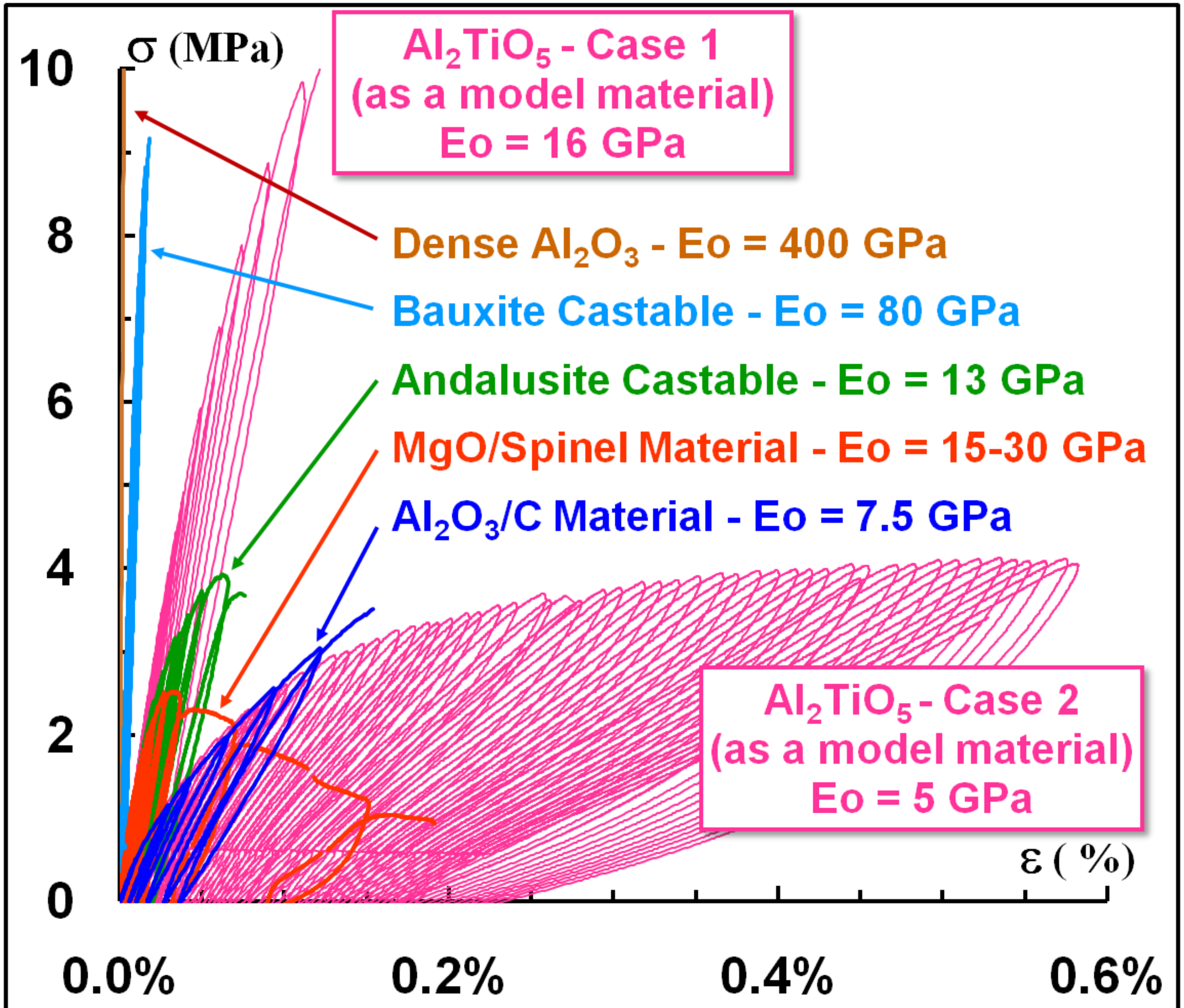

➔ Inspiration for other heterogeneous materials

➔ **Promote flexibility (high strain** du rupture ε_r, high work of fracture G_f)

➔ Some guideline for microstructure design in order to improve these properties

Université de Limoges

CNRS

SPCTS Science des Procédés Céramiques et de Traitements de Surface
UMR CNRS 7315

Strain field measurement : Digital Image Correlation (DIC)

Full kinematic field

Numerical model validation

❖ Simulated and experimental strain field

Parameter identification

❖ Inverse methods : FEMU, FEMU-R

Refined mechanical characterization

❖ Highlighting non-linear mechanical behaviour

❖ Crack detection and process zone evolution

❖ Fracture behavior characterisation

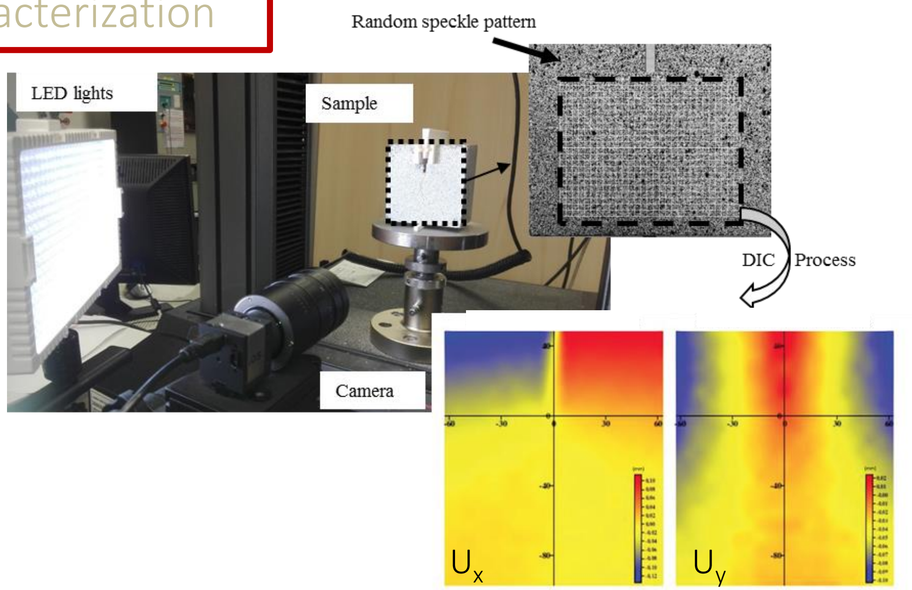

Displacement field

Digital Image Correlation (DIC)

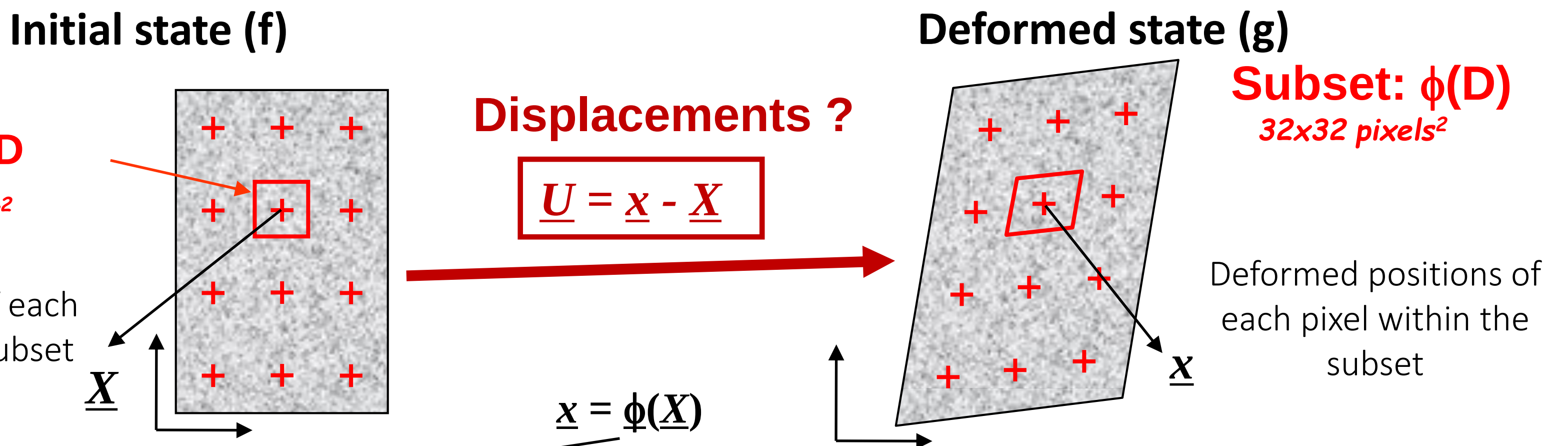

Material Transformation ϕ

Translation + Homogeneous local gradient of displacement

$$\phi(\underline{X}) = \underline{X} + \underline{T} + \frac{\partial U(\underline{X}_0)}{\partial \underline{X}}(\underline{X} - \underline{X}_0)$$

Looking for unknown local data of displacement…

➔ best values of

$$\underline{q} = \left(u, v, \frac{\partial u}{\partial x}, \frac{\partial u}{\partial y}, \frac{\partial v}{\partial x}, \frac{\partial v}{\partial y} \right)$$

Correlation Coefficient: $C(\underline{q}) = \sum_{\underline{X} \in D} c(\underline{q})^2$

working with grey levels of each pixel within the subset

$$c(\underline{q}) = \frac{f(\underline{X})}{\overline{\overline{f(\underline{X})}}} - \frac{g(\phi(\underline{X}))}{\overline{\overline{g(\phi(\underline{X}))}}}$$

… which minimize: $C(\underline{q})$

Mean square minimization by Bi-linear Interpolation of g for sub-pixel accuracy

Strain calculated by finite differences from 4 adjacent subsets (l_0 distance between subsets)

- ✓ Choice of a given threshold ε_s (just above the background noise)
- ✓ If $\varepsilon > \varepsilon_s$ then strain corresponds locally to a crack

Drawbacks :

- **Hypothesis of "continuous material" in DIC calculations (material transformation ϕ and strain calculations)**
- **Rather bad spatial resolution of cracks due to gauge length l_0 coming from inter subset positions**

Two-Parts Digital Image Correlation (2P-DIC)

Initial state (f)

Deformed state (g)

Subset: D
64x8 pixels²

Initial positions of each pixel within the subset

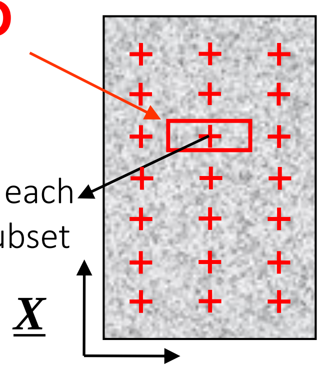

Displacements ?

$\underline{U} = \underline{x} - \underline{X}$

$\underline{x} = \phi(\underline{X})$

Locally treated in 2 parts

$\underline{\phi}(\underline{X}) = \underline{\phi}_1(\underline{X}_1) + \underline{\phi}_2(\underline{X}_2)$

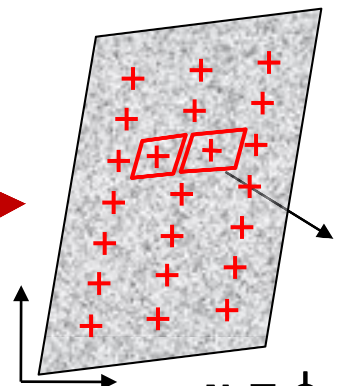

Subset can be locally divided into 2 parts: $\phi_1(D_1)$ and $\phi_1(D_2)$

Deformed positions of each pixel within the 2 subsets

$\underline{x}_1 = \phi_1(\underline{X}_1)$ **and** $\underline{x}_2 = \phi_2(\underline{X}_2)$

Rectangular subset
Vertical direction
No local strain

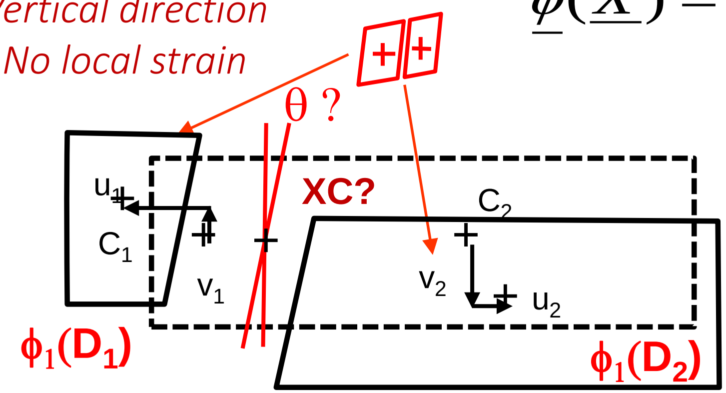

$\underline{q}_1 = (u_1, v_1)$ $\underline{q}_2 = (u_2, v_2)$

$XC \in [-N/4;N/4]$

$\theta \in [-\pi/3;\pi/3]$

➔ Best values of XC, θ and $\underline{q}_1$ and $\underline{q}_2$

Pseudo strain calculation:

$$\varepsilon = \frac{2\sqrt{(n/2+u_2-u_1)^2+(v_2-v_1)^2}}{n} - 1$$

✓Threshold used to discriminate crack occurrence from measurement noise

✓Automatic crack measurement procedure

Digital Image Correlation (DIC): Observation of process zone evolution

- Choice of a given threshold (just above the background noise) ε_s: here about 0.002
- If $\varepsilon > \varepsilon_s$ then strain corresponds locally to a crack

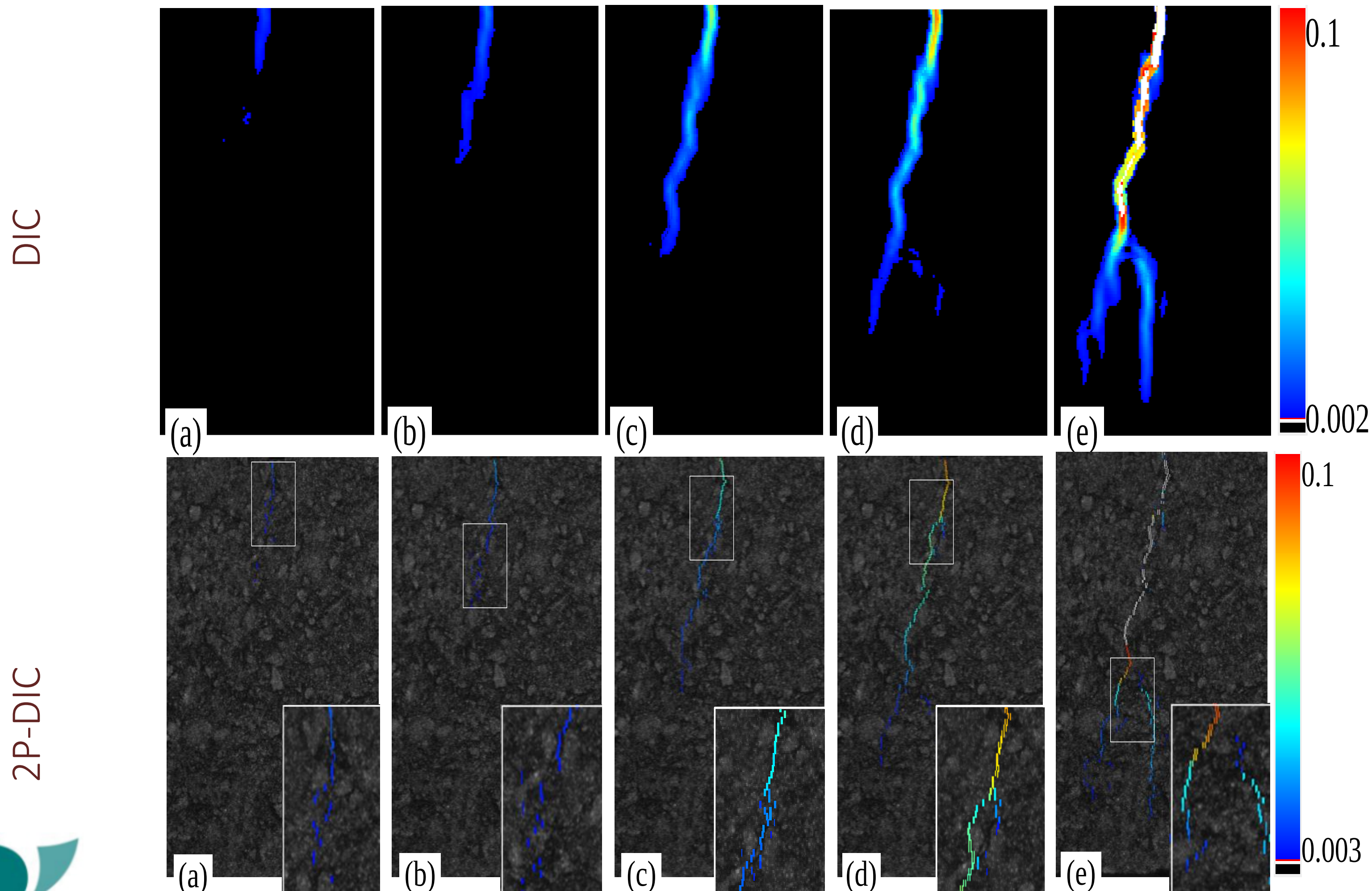

Discrete element method (DEM)

- Discrete Element Method was initiated by CUNDALL and STRACK in the early 80’s * to simulate granular media

  - ✓ Discrete elements mimic a non-deformable body
  - ✓ Discrete elements are in interaction by contacts law

Granular DEM simulation

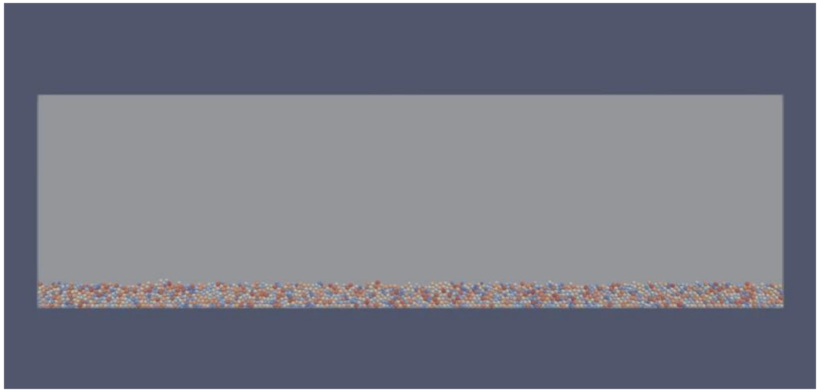

- Recently, this method was adapted to simulate continuous media (concrete, rock, ceramic, etc.)

  - ✓ Discrete elements mimic a non-deformable body.
  - ✓ Discrete elements are in interaction by cohesive bonds
  - ✓ Cohesive bonds could be broken.

DEM simulation of ceramic cracking

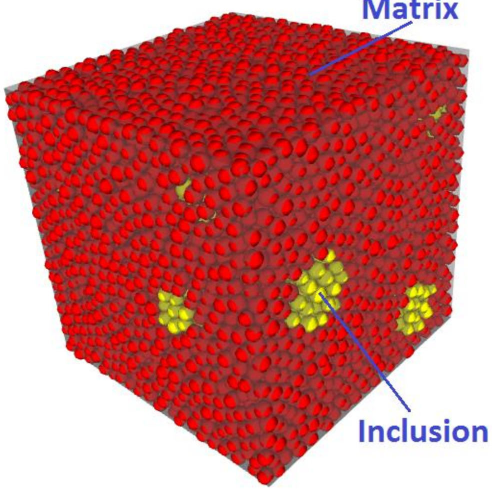

** CUNDALL, P. A. et O. D. L. STRACK (1979). “A discrete numerical model for granular assemblies”. In : Geotechnique 29, p. 47–65.1979.29.1*